https://doi.org/10.5194/egusphere-2022-787
Preprint. Discussion started: 26 August 2022

Millennial hydrological variability in the continental northern Neotropics during MIS3-2 inferred from sediments of Lake Petén Itzá, Guatemala

Rodrigo Martínez-Abarca[1*], Michelle Abstein[1], Philipp Hoelzmann[2], David Hodell[3], Mark Brenner[4], Steffen Kutterolf[5], Sergio Cohuo[6], Laura Macario-González[7], Mona Stockhecke[8], Jason Curtis[4], Flavio Anselmetti[9], Daniel Ariztegui[10], Thomas Guilderson[11,12], Alexander Correa-Metrio[13,14], Frederik Schenk[15,16], Thorsten Bauersachs[17], Liseth Pérez[1], and Antje Schwalb[1]

[1]Institut für Geosysteme und Bioindikation, Technische Universität Braunschweig, Braunschweig, 38106, Germany
[2]Institut für Geographische Wissenschaften, Physische Geographie, Freie Universität Berlin, Berlin, 12249, Germany
[3]Godwin Laboratory for Palaeoclimate Research, Department of Earth Sciences, University of Cambridge, Cambridge, CB2 3EQ, UK
[4]Department of Geological Sciences and Land Use and Environmental Change Institute, University of Florida, Florida, 32611, USA
[5]GEOMAR Helmholtz Centre for Ocean Research Kiel, Kiel, 24148, Germany
[6]Tecnológico Nacional de México/I.T. de Chetumal, Chetumal, 77013 Mexico
[7]Tecnológico Nacional de México/I.T. de la Zona Maya, Quintana Roo, 77013 Mexico
[8]Large Lakes Observatory (LLO), University of Minnesota-Duluth, Minnesota, 55812, USA
[9]Institute of Geological Sciences and Oeschger Centre for Climate Change Research, University of Bern, Bern, 3012, Switzerland
[10]Department of Earth Sciences, University of Geneva, Geneva, 1205, Switzerland
[11]Center for Accelerator Mass Spectrometry, Lawrence Livermore National Laboratory, California, 94550, USA
[12]Ocean Sciences Department, University of California–Santa Cruz, California, 95064, USA
[13]Instituto de Geología, Universidad Nacional Autónoma de México, Mexico City, 04510, Mexico
[14]Centro de Geociencias, Universidad Nacional Autónoma de México, Juriquilla, 76230, Mexico
[15]Department of Geological Sciences and Bolin Centre for Climate Research, Stockholm University, Stockholm, 11418, Sweden
[16]Department of Geosciences and Geography, University of Helsinki, Helsinki, FI-00014, Finland
[17]Institute of Geosciences, Organic Geochemistry Group, Christian-Albrechts-University, Kiel, 24118, Germany

Correspondence to: Rodrigo Martínez-Abarca (l.martinez-abarca@tu-bs.de)

Abstract. We inferred hydrological changes in Lake Petén Itzá (Guatemala) during Marine Isotope Stages (MIS) 3-2 using geochemical (Ti, Ca/Ti+Al+Fe ratio and Mn/Fe) and mineralogical (carbonates, gypsum, quartz, clay) data from sediment core PI-2 to reconstruct changes in runoff, lake evaporation, organic matter sources and potential oxic/anoxic conditions associated with variations in water-level during the last ~59 cal ka BP. Early MIS3 (57.0-52.5 cal ka BP) was dominated by relatively wet conditions, higher lake primary productivity and anoxic waters, which persisted into the subsequent interval (52.5-39.0 cal ka BP), except for two periods of possible low water-level at 52 and 46 cal ka BP when our data suggest higher evaporation, high terrestrial organic matter input and persistent oxic conditions. Towards the end of MIS3 and start of MIS2 (39.0-23.0 cal ka BP), lake evaporation increased considerably, as did inputs of terrestrial organic matter, and waters became more oxic as water-levels dropped and the site moved from the hypolimnion to the epilimnion. These conditions reversed during the Last Glacial Maximum (23.0-18.0 cal ka BP) when runoff and lake productivity increased and waters again became anoxic as a result of rising water-levels. Refining the age-depth model for the Site PI-2 also allowed the correlation to Greenland Interstadials (GI14-2), Greenland Stadial (GS14-2) and Heinrich Stadials (HS5-1). HS and GS were characterized by increases in Ca/Ti+Al+Fe ratios

https://doi.org/10.5194/egusphere-2022-787
Preprint. Discussion started: 26 August 2022

and gypsum content generally indicative of drier conditions. GS13, 9 and 5 showed the driest conditions associated with the contemporaneous establishment of HS5-3, respectively. In contrast, GI show high Ti values which suggests relatively greater runoff and overall wetter conditions compared with GS and HS, with the most marked GI peaks between 40 and 30 cal ka BP. This runoff variability is in accord with shifts in the average position of the Intertropical Convergence Zone and strength of the Atlantic Meridional Oceanic Circulation during the Late Pleistocene.

1 Introduction

The last glacial period (115-11 cal ka BP) in the high latitudes of the northern hemisphere was marked by strong millennial-scale climate variability. Marine Isotope Stages (MIS) 3 (57-29 cal ka BP) and the last deglaciation (19-10.5 cal ka BP) were characterized by abrupt climate events. In the Greenland ice core, these are referred to as Dansgaard-Oeschger (D/O) events (Dansgaard et al., 1993) and consist of rapid oscillations between cold Greenland stadial (GS) and warm interstadial (GI) conditions. During some of the most extreme Greenland stadials, North Atlantic marine sediment cores were found to contain layers of ice-rafted detritus (IRD) rich in detrital carbonate derived from Paleozoic bedrock underlying Hudson Strait (Heinrich, 1988; Broecker et al., 1992; Hemming, 2004). These so-called "Heinrich events" were attributed to massive discharges of the Laurentide Ice Sheet to the North Atlantic via Hudson Strait. Greenland stadials (GS) that contain Heinrich events are referred to as Heinrich stadials (HS). Freshwater forcing associated with Heinrich events weakened the Atlantic Meridional Overturning Circulation (AMOC) and the Intertropical Convergence Zone (ITCZ) moved south, resulting in tropical hydroclimate events in the low latitudes (Bradley and Diaz, 2021).

Lake Petén Itzá, northern Guatemala (Fig. 1), is located in a highly biodiverse and geographically sensitive climate area that is affected by the annual migration of the ITCZ, trade wind intensity and moisture transport from the Caribbean Sea. The sediments of this lake contain one of the oldest records in the region (75 kyr). Only a few nearby records in the northern Neotropics exceed 100 thousand years in age (e.g. Lake Chalco, Central Mexico; Martínez-Abarca et al., 2021a). For these reasons, Lake Petén Itzá has a unique sediment record with which to study abrupt climate change for stadial-interstadial events during MIS3-2. In earlier studies of the Lake Petén Itzá's sediments, the identification of these events was based mainly on the presence of gypsum and clay layers as described by Hodell et al., (2008) and Mueller et al., (2010). Subsequent work has been conducted including stable isotope geochemistry (Escobar et al., 2012; Hodell et al., 2012; Grauel et al., 2016; Mays et al., 2017), as well as biological indicators of climate change such as ostracods (Cohuo et al., 2018, 2020; Pérez et al., 2021), pollen and charcoal (Correa-Metrio et al., 2012). During HS, a drop-in mean annual air temperature between 6 and 10°C compared with modern values has been reconstructed in the region (Hodell et al., 2012). Additionally, Lake Petén Itzá may have a reduction of up to 3°C in the mean water-temperature according with recent ostracods-based transfer function (Cohuo et al. 2018; Pérez et al., 2021). High salinities associated with a shallow lacustrine environment have been reconstructed based on ostracods data suggesting drier conditions. Moreover, stable isotope geochemistry reveals low lake levels during HS that caused Site PI-6 (water depth 71 m) to be within the epilimnion where oxygen concentrations are high (Escobar et al., 2012). These cold and dry environments promoted the establishment of savanna vegetation such as Poaceae and Acacia, as well as littoral ostracods species as *Cytheridella ilosvayi* and *Paracythereis opesta* dominated the assemblage. During GS, annual air temperature was between 19 and 20°C (Correa-Metrio et al., 2012) i.e. 6°C less than the modern annual

https://doi.org/10.5194/egusphere-2022-787
Preprint. Discussion started: 26 August 2022

atmospheric temperature in the region, accompanied by a high fire-activity around the lake. This body of work at Lake Petén Itzá indicates that millennial change in climate and vegetation of Petén Itzá varied in concert with conditions in the North Atlantic expressed, such that colder, drier stadials (especially Heinrich stadials) and warmer, wetter interstadials occurred in Petén Itzá.

Despite the abundant environmental and paleo-climate information regarding MIS3-2 gleaned from Lake Petén Itzá sediment records, responses of the lake to changes in runoff and evaporation, and related shifts in redox conditions have been analyzed mainly in only one of the seven cores drilled in Petén Itzá (Site PI-6; 71 water depth). Here we investigated Site PI-2, located 4 km to the east of Site PI-6 and in a water depth of 54 m, to test if the hydroclimate signals inferred from Site PI-6 were pervasively recorded in sediments throughout the lake.

The aim of this study is to investigate the hydrological response of Lake Petén Itzá to climate and environmental changes at Site PI-2 in the eastern lake basin (Fig. 1). We established an updated chronology for the sediment record from Site PI-2 in Lake Petén Itzá using existing AMS ^{14}C dates and non-linear age modeling. Moreover, we used high-resolution geochemical and mineralogical data to reconstruct hydrological changes for MIS 2 and 3 (59 to 15 cal ka BP) including millennial climate oscillations such as HS, GI and GS. Results are compared with previous studies of Site PI-6.

2 Study area

Lake Petén Itzá is located in the northern lowlands of Guatemala (16°59'39.90"N, 89°49'21.07"W, 110 m above sea level [m asl]; Fig. 1). It has a surface area of ~100 km^2 and a maximum depth of 165 m (Hodell et al., 2006). The region has a humid tropical climate ("Af" according to the Köppen classification), with mean monthly air temperatures ranging from 22 to 30°C (INSIVUMEH, 2021). Mean annual precipitation is ~1600 mm (INSIVUMEH, 2021), but varies intra-annually, with a pronounced dry season from January to May, and a wet season that extends from late May through December. Maximum rainfall typically occurs in September, associated with tropical storms and hurricanes. The annual rainfall cycle is driven by the annual cycle of the latitudinal migration of the ITCZ, with dry conditions during winter when it is in the most southerly position, and wet conditions during summer when it is farther north. The region is also strongly influenced bythe NE Trade Winds that transport heat and moisture westward from the Atlantic toward the Caribbean Sea (Mestas-Nunez et al., 2005; Hodell et al., 2008).

The lake lies in a basin formed by asymmetric faulting (Fig. 1). To the north, marine carbonates of Paleocene-Eocene age outcrop, whereas to the south the surface rock is composed of Cretaceous limestones (IGN, 1970). To the southeast, rocks as well as Quaternary sediments and soils of alluvial origin dominate, the latter two consisting mainly of carbonates and clays (Simmons et al., 1959; IGN, 1970; Mueller, 2009). The karst geology of the area promotes rapid infiltration of rainfall into the groundwater (Hodell et al., 2008), although an ephemeral stream at the southeast end of the lake transports water and sediment to the waterbody during the rainy season.

https://doi.org/10.5194/egusphere-2022-787
Preprint. Discussion started: 26 August 2022

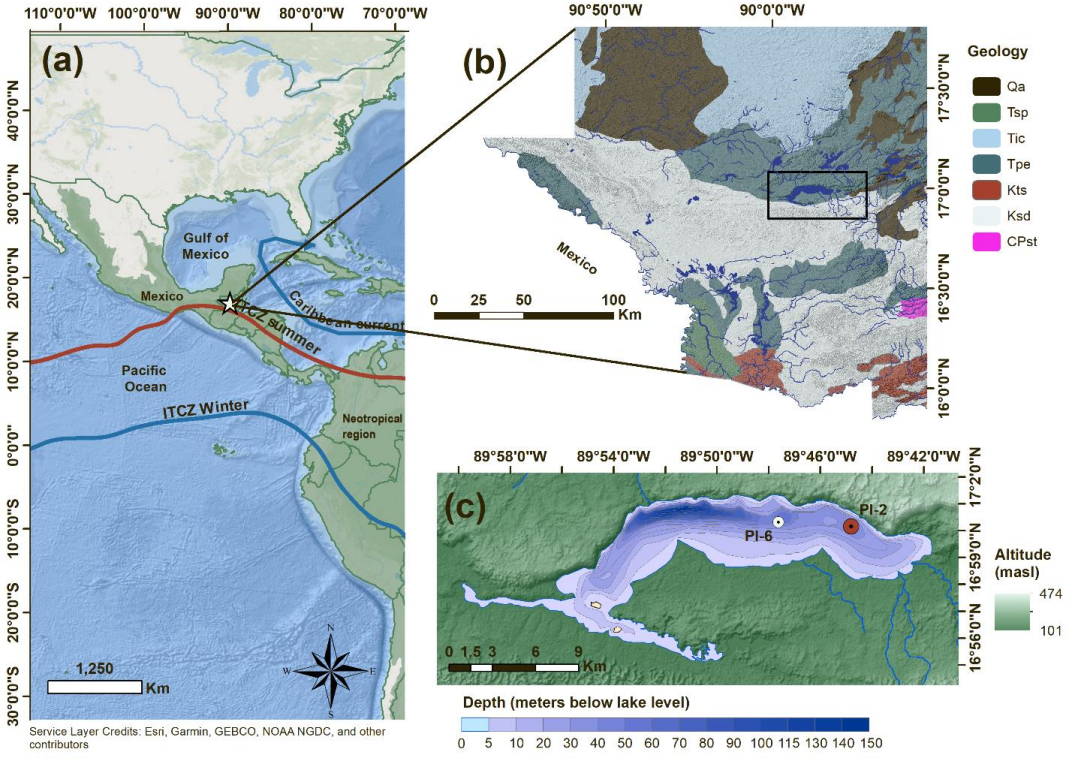

Figure 1. Geographic map with the location of Lake Petén Itzá. A) Location of Guatemala in Central America and geographic position of the lake (white star). The Neotropical region is shown in green. ITCZ positions during summer and winter are shown. The warm Caribbean surface current is indicated. Service Layer Credits: Esri, Garmin, GEBCO, NOAA NGDC, and other contributors (2022). B) Geology and hydrology of the Petén Itzá region. The black rectangle indicates the position of Lake Petén Itzá. Qa) Quaternary alluvium, Tsp) Tertiary upper Oligocene-Pliocene, Tic) Eocene sedimentary rocks, Tpe) Paleocene-Eocene marine sediments, Kts) Cretaceous-Tertiary clastic sediments, Ksd) Cretaceous carbonaceous rocks, CPst) Carboniferous-Permian sand conglomerate (geological information: IGN, 1970). C) Digital elevation model around the lake, principal fluvial streams and bathymetry of Petén Itzá, the PI-2 location is indicated by the red dot while PI-6 by the white point.

3 Methods

3.1 ICDP drilling campaign

During February and March 2006, multiple cores were drilled at seven locations in Lake Petén Itzá (PI-1, PI-2, PI-3, PI-4, PI-6, PI-7 and PI-9) as part of an International Continental Scientific Drilling Program (ICDP) project. The maximum drilling depth reached 133 m at Site PI-7. Sediment lithology, magnetic susceptibility and density data for the cores were presented by Hodell et al., (2006, 2008) and Mueller et al., (2010). Here, we focus on the sediment sequence recovered from Site PI-2. The site displayed a relatively high mean sedimentation rate (~150 cm ka^{-1}; Kutterolf et al., 2016) and average sediment core recovery of 86.3%, which permitted the reconstruction of climate change at high temporal resolution. PI-2 was retrieved from a water depth of 54 m in the eastern part of the lake

https://doi.org/10.5194/egusphere-2022-787
Preprint. Discussion started: 26 August 2022

(16°59'58.04"N, 89°44'41.51"W, Fig. 1C). The drill site receives detrital material in the form of colluvium that comes off the steep north shore. Five holes were drilled at Site PI-2, which reached a maximum sediment depth of ~82 m. The composite sequence at Site PI-2 was divided into 11 lithostratigraphic units based on changes in facies composition (Mueller et al., 2010). For this study, we analyzed sediment samples from Units 6 to 2 (67-19 m depth), which span the interval of MIS3-2 (Correa-Metrio et al., 2012; Escobar et al., 2012).

Table 1. AMS ^{14}C dates and ages of tephra used for the age-depth model. Data with an asterisk (*) are measurements of terrestrial organic matter (i.e. woody debris) reported by Mueller et al., (2010). Data with double asterisk (**) are tephras reported by Kutterolf et al., (2016). All radiocarbon dates were calibrated using a Bayesian model (Blaauw and Christen, 2011) and the IntCal20 curve (Reimer et al., 2020). "avg" refers to the mean age obtained from two dates in the same sample.

labID	Site-Core, cm	Depth (m)	Age (^{14}C a)	± (1σ)	Mean (cal BP)	Modelled age range (cal BP)
144277*	2D-1H-1, 14	0.22	425	30	22	-60 – 150
139341*	2D-2H-2, 25	4.88	1715	35	1620	1516 – 1737
139342_avg*	2B-4H-2, 39	10.25	3740	33	4043	3655 – 4169
144270*	2A-5H-1, 87	10.85	4280	30	5203	4903 – 5288
139344_avg*	2B-5H-1, 102	12.45	7468	40	8276	8170 – 8390
139346*	2D-5H-1, 56	12.76	7835	30	8736	8614 – 8875
139399*	2B-6H-2, 41	16.43	11135	40	13057	12909 – 13168
139399*	2D-6H-2, 44	17.46	11880	35	13637	13439 – 13792
144272*	2A-8H-1,96	20.44	13095	40	15710	15497 – 15907
139400*	2D-8H-1, 5	21.65	13480	45	16197	16059 – 16326
139401_avg*	2B-8H-1, 132	22.24	13533	45	16408	16225 – 16600
139402*	2B-9H-1, 146	25.47	15355	50	18632	18321 – 18820
144274*	2B-10H-2, 98	29.59	19740	70	23904	23535 – 24236
144269*	2A-12H-1, 47	31.49	21940	80	26176	25932 – 26661
139403*	2B-12H-1, 121	38.41	25540	160	35488	32614 – 37722
139404*	2A-14H-1, 115	40.38	32680	980	36947	34181 – 38962
139405*	2A-16H-1, 66	44.55	34380	450	39794	38469 – 40926
139406*	2C-2H-1, 135	47.08	38760	740	42621	41955 – 43422
139407*	2A-17H-1, 104	48.06	41350	1020	43944	42974 – 44960
139343*	2A-17H-1, 151	48.4	41600	900	44195	43186 – 45263
C1**	2B-5H-2, 65	13.09	9805	100	9378	9231 – 9550
C2**	2A-7H-1, 131	17.69	13158	100	13761	13537 – 13959
C4**	2A-19H-2, 10	54.46	49100	2000	48793	45957 – 52137
C5**	2C-9E-1, 114	64.22	53000	3000	55826	51080 – 62132

3.2 Age-depth model

Previous studies established different chronologies for the Lake Petén Itzá sediment sequences, with a focus on the composite section from Site PI-6. These studies used linear interpolation between radiocarbon dates (Hodell et al., 2008; Mueller et al., 2010), projection onto the PI-6 sequence of AMS ^{14}C dates from other cores (Escobar et al., 2012), and dates of tephra layers (Kutterolf et al., 2016). Mays et al., (2017) constructed a Bayesian age model for Site PI-6.

https://doi.org/10.5194/egusphere-2022-787
Preprint. Discussion started: 26 August 2022

We similarly refined the age-depth model for PI-2 using a Bayesian model (Blaauw and Christen, 2011). In this model (PETEN 02), we used 20 radiocarbon ages reported by Mueller et al., (2010) and Escobar et al., (2012), together with four dated tephras preserved in the PI-2 sequence (Kutterolf et al., 2016; Table 1). Radiocarbon ages were calibrated using the IntCal20 curve (Reimer et al., 2020). The model was established using the Bacon package (Blaauw and Christen, 2011) in the R-Studio software (v. 4.2). An initial sedimentation rate of 1 mm yr^{-1} (100 cm ka^{-1}) and 28 segments along the core were assumed. Processes that deposit material rapidly at the bottom of the lake, such as turbidite flows and volcanic ashfalls, can confound the chronology by contributing substantial amounts of material in a short time (Moernaut et al., 2017; Mulder et al., 2019). Hence, we excluded 31 such deposits during the modeling, including carbonaceous turbidites and tephras, identified using the descriptions of Mueller et al., (2010) (Appendix A).

3.3 X-Ray fluorescence (XRF)

X-Ray fluorescence measurements were carried out at the University of Minnesota, Duluth, using a Cox Analytical Itrax Core Scanner (Cr-Tube, 30 kV, 55 mA, 15 s exposure) with a resolution of 1 cm. Particular focus was given to titanium (Ti), aluminum (Al), calcium (Ca), iron (Fe) and manganese (Mn) because they are suitable indicators of runoff, evaporation and redox conditions. Data from XRF as counts per second (cps) were calibrated using a log-ratio calibration following Weltje and Tjallingii (2008) and Weltje et al., (2015). Log-ratio calibration incorporates uncertainties acquired during core scanning such as the water content in the sediment, grain size and irregularities in the sediment surface (Dunlea et al., 2020). For each XRF measurement, we divided an element (e.g. $Ti_{(cps)}$) by a common denominator that was measured simultaneously in the XRF spectra (e.g. $Ti_{(cps)}/Inc_{(cps)}+Coh_{(cps)}$). We selected the sum of the Incoherent and Coherent scattering as the common denominator because they reflect changes in the water content and density of the sediments (Kylander et al., 2011; Marshall et al., 2011). The natural logarithm of the ratio was then calculated [e.g. $\ln (Ti_{(cps)}/Inc+Coh_{(cps)})$]. Calibration was carried out using Xelerate software (Bloemsma, 2015; Weltje et al., 2015). Data as cps and log-ratio calibrated can be found in the Appendix B. A LOESS smoothing function was applied to dampen the noise signal from measurement errors or anomalous data. LOESS smoothing was carried out in R-Studio (v. 4.2) (R Core Team, 2018) with a span of 3.

3.4 X-Ray Diffraction (XRD)

To document changes in sediment mineralogy, 100 samples were used for X-ray diffraction (XRD) analysis. Sampling was carried out at irregular intervals ranging from 0.5 to 1.0 m. Sediment samples were dried at room temperature and ground with a mortar and pestle. Measurements were conducted with a Rigaku Miniflex 600 (15mA/40kV) XRD at the Department of Physical Geography, Freie Universität Berlin. Peaks obtained from 3 to 80° of rotation were identified with X-Pert High Score (Version 1.0b) from Philips Analytical. The peaks were calibrated against the main quartz peak (I100) at d=3.34 Å. Diffraction potential files of the International Center for Diffractometric Data, USA, were used as reference for the identification of the different mineral phases. The quartz and gypsum counts, the sum of montmorillonite+vermiculite (clay) and the sum of calcite+dolomite+aragonite+magnesium calcite (carbonate) were summed and the relative percentages were calculated as follows: Mineral [%] = (Mineral count*100)/Σ Minerals (Last, 2001).

https://doi.org/10.5194/egusphere-2022-787
Preprint. Discussion started: 26 August 2022

3.4 Bulk-geochemical measurements

Analyses of total carbon (TC), total organic carbon (TOC), total inorganic carbon (TIC) and total nitrogen (TN) were carried out on the same sediment samples used for XRD. All measurements were performed at the Department of Geological Sciences, University of Florida, Gainesville. TC and TN were determined with a Carlo Erba NA1500 CNHS Elemental Analyzer. TIC was measured coulometrically (Engleman et al., 1985) with a UIC CO_2 coulometer 5011 (Coulometrics) coupled with an AutoMate preparation device. TOC was calculated as the difference between TC and TIC. TOC/TN ratios are reported on a molar basis.

4 Results

4.1 Chronology

Data presented in this study cover the depth interval from 67 to 19 m of the PI-2 record, corresponding to an age range from 59 to 15 cal ka BP (Fig. 2). From the surface to 51 m depth, average age uncertainty is ±0.8 ka. The uncertainty of the chronology increases in the deepest sediment interval, especially below 51 m depth (>46 cal ka BP), reaching ±6.7 ka at the bottom of the sequence (67 m depth). There were two intervals during which instantaneous deposits (mainly carbonaceous turbidites) were abundant: between 67 and 48 m depth (58.5-43.8 cal ka BP) and from 23 to 0 m depth (16.6-0 cal ka BP). Our age-depth model differs from the one in Kutterolf et al., (2016) mainly in the interval between 40 and 34 cal ka BP, where ages calculated by our model are as much as 2 ka younger. However, this is within the average uncertainty of our age model at these depths (±2.3 ka).

4.2 Climate proxies

Results are presented by age and according to the lithostratigraphic units proposed by Mueller et al., (2010; Table 2). Ti log-ratio values vary between -5.6 (low runoff) and -1.2 (high runoff) throughout the sequence, with an average of -2.2±0.7 (Fig. 3). In Units 6 and 5, Ti is characterized by fluctuating values compared to the rest of the sequence, in which values range between -5.6 and -1.2. Lowest average values (≤ -2.8) were observed in Unit 4. Units 3 and 2 display the highest Ti content, both with maxima of -1.3.

$CaCO_3$ data obtained by XRD vary from 4.2 to 75%, with an average of 33.9±15.3%. Units 6 and 5 show similar values of $CaCO_3$ oscillating between 8.7% and 73.4% (mean 40.7±12.4%). A reduction in the CaCO3 content characterizes Unit 4 reaching up an average of 28.9±14.9%. In Unit 3, data vary from 26.3% and 58.7% (mean = 34.7±7.5%). During Unit 2, a slight average decrease (mean = 20.9±17.9%) dominates, finishing with a peak up to 75% at 15.5 cal ka BP.

Ca/Ti+Al+Fe log-ratios range from 0.1 (low evaporation) to 6.3 (high evaporation) throughout the sequence, with an average of 2.8±1.0 (Fig. 3). In Units 6 and 5, Ca/Ti+Al+Fe ratios are variable (0.7 to 5.6), with three pronounced peaks of 4.9 (51.9 cal ka BP; 58.9 m), 5.6 (46.1 cal ka BP; 50.8 m) and 4.8 (40.3 cal ka BP; 45.3 m). The ratio increases in Unit 4 and range from 1.4 to 6.3 (mean = 3.4±0.7). Unit 3 displays the lowest Ca/Ti+Al+Fe ratios, varying between 0.6 and 3.3 (mean = 1.7±0.4). Unit 2 is characterized by highly variable Ca/Ti+Al+Fe ratios, ranging between 0.1 and 6.0 (mean = 3.2±1.4), and shows highest ratios <6.0 at the top of the sequence.

https://doi.org/10.5194/egusphere-2022-787
Preprint. Discussion started: 26 August 2022

The mineralogical composition of the Lake Petén Itzá record obtained by XRD is dominated by carbonates, including calcite, dolomite, aragonite and magnesium calcite. About 65% of the sediment samples contained more than 50% carbonate, with calcite (mean 45.9±27.8%) and dolomite (mean 13.4±13%) being most common. Quartz shows highest average values in Units 6 (3.0±1.5%), 5 (3.2±2.0%) and 3 (5.1±2.5%). The clay content (montmorillonite+vermiculite) is highly variable throughout the record, ranging from 0 to 13.7% (mean 3.6±3.0%). It shows a gradual decrease from Unit 6 (4.5%) to Unit 4 (2.1%). Unit 3 contains the highest clay content (mean 8.5±2.9%), but decreases upward to an average of 1.9% in Unit 2. The gypsum content is highly variable and ranges from 0 to 100%, with an average of 32.6±36.0% (Fig. 3). Units 6, 5 and 3 show the lowest gypsum content of the record, with average values of 5.1, 14.9 and 6.2%, respectively. In Unit 5, maxima of 96.8 and 77.7% occur at 50.9 cal ka BP (56.8 m) and 46.3 cal ka BP (51.1 m), respectively. In Units 4 and 2, there is a strong increase in the gypsum content, with average values of 53.9 and 78.2%, respectively.

TOC values vary between 0.2 and 6.1%, with an average of 2.1±1.1% throughout the sequence (Fig. 3). TOC values range from 1.1 to 4.5% in Unit 6. Unit 5 displays TOC values that range from 0.5 to 6.1%, and significantly decrease around 47.2 cal ka BP (52.3 m). From 37.8 to 30.9 cal ka BP (42.0 to 35.0 m depth) in Unit 4, three distinct maxima with TOC values of 3.7% (37.3 cal ka BP; 41.1 m), 5.2% (35.4 cal ka BP; 38.4 m) and 3.4% (33.0 cal ka BP; 36.5 m) were determined. The TOC content in Unit 3 increases to a maximum of 3.7%, with an average of 2.2±0.6%. Unit 2 is characterized by lower TOC values, which vary from 0.2 to 2.5% (mean 0.7±0.4%).

Molar TOC/TN ratios range from 4 (high aquatic organic matter content) to 38 (high terrestrial organic matter content) throughout the record (mean 16.8±6.3). Unit 6 shows TOC/TN ratios that average 10.7±3.2, with a gradual increase to 18.9 at the top of the unit (Fig. 3). Units 5 and 4 display similar TOC/TN ratios, ranging between 4.4 and 38. Four maxima of 31.3 (51.8 cal ka BP; 58.6 m), 35.9 (46.4 cal ka BP; 51.0 m), 27.4 (40.4 cal ka BP; 45.3 m) and 38 (31.9 cal ka BP; 35.7 m) were identified, as were minima of ~6.8 between 40.3 and 39.2 cal ka BP (45.2-43.9 m depth). At the top of Unit 4 (31.0-23.4 cal ka BP; 35.0-29.0 m depth), TOC/TN ratios decrease gradually from 26.1 to 10.8. Units 3 and 2 have the lowest values of the entire sequence, ranging between 4.6 and 17.5, with a slight increase to 20.9 at the top of Unit 2.

Mn/Fe log-ratios range between -5.5 (rather anoxic) and -1.3 (rather oxic), with an average of -3.4±0.5 throughout the record (Fig. 3). Unit 6 displays the lowest values of the sequence varying between -4.2 and -2.7. Unit 5 presents a gradual increase in the Mn/Fe ratios between 52.7 and 46.1 cal ka BP (60.0-50.8 m) reaching up to -1.3. Units 5 and 4 show similar values, which vary from -5.5 to -1.3, with maxima of -1.3 (46.1 cal ka BP; 50.8 m), -2.1 (40.3 cal ka BP; 45.3 m), -1.9 (37.1 cal ka BP; 40.5 m) and -1.7 (29.6 cal ka BP; 34.3 m). Units 3 and 2 values fluctuate between -4.5 and -3.1 (-3.7±0.3).

https://doi.org/10.5194/egusphere-2022-787
Preprint. Discussion started: 26 August 2022

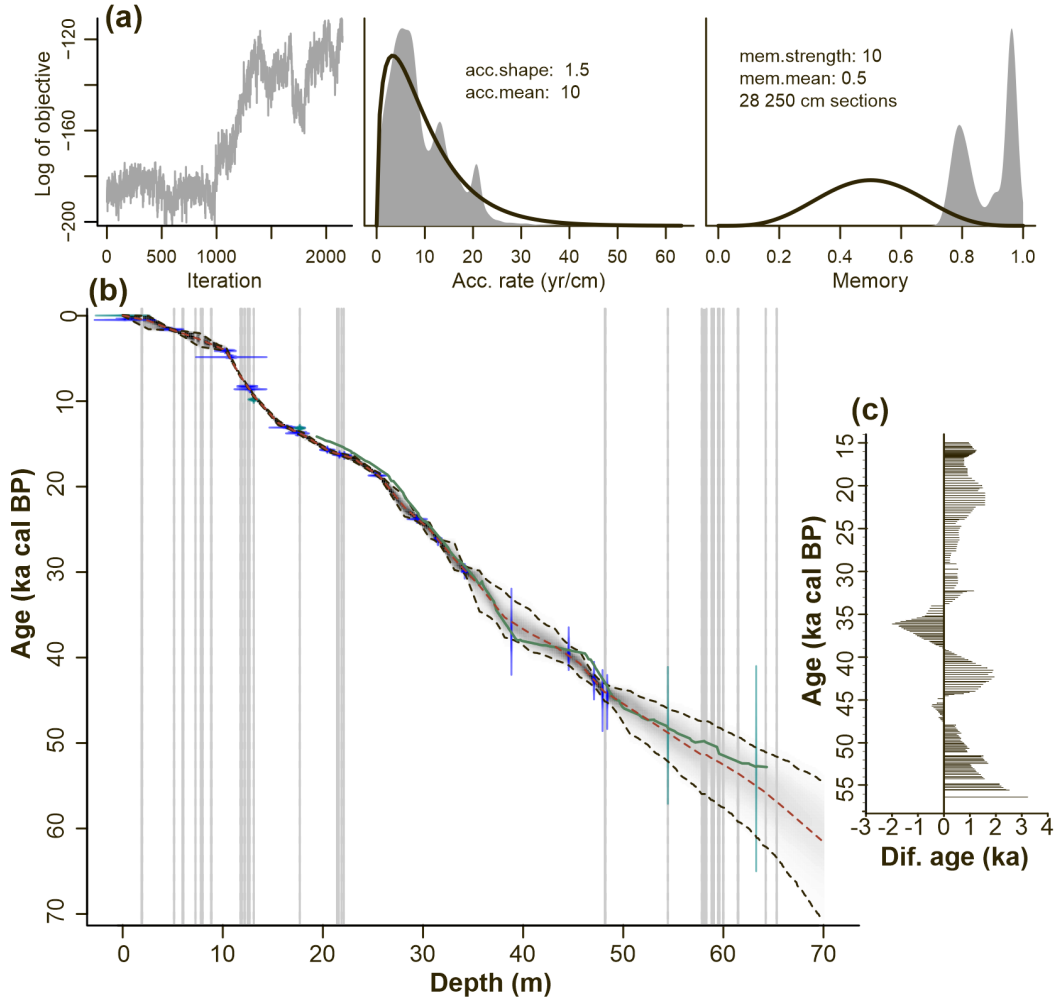

220 **Figure 2.** Age-depth model obtained for the PI-2 record: A) Model parameters estimated by (from left to right) the quantity of iterations in each section, range of accumulation rate and memory (how much the accumulation rate of a particular depth in the core depends on the depth above it; 1=100% memory); B) Chronology of the PI-2 record. Gray vertical lines indicate the location of the 32 instantaneous deposits. Ages and their uncertainties are indicated in blue. Red-solid line shows the chronology obtained by Kutterolf et al., (2016) and used in Cohuo et al., (2018, 2020). Red-dotted line represents the average age, while black-dotted line
225 is the minimum and maximum range of each age. C) Age difference between the models of this study and the one presented by Kutterolf et al., (2016) between 59 and 15 cal ka BP. The data were calculated as follows: Dif. Ages = Ages this study - ages reported by Kutterolf et al., (2016).

https://doi.org/10.5194/egusphere-2022-787
Preprint. Discussion started: 26 August 2022

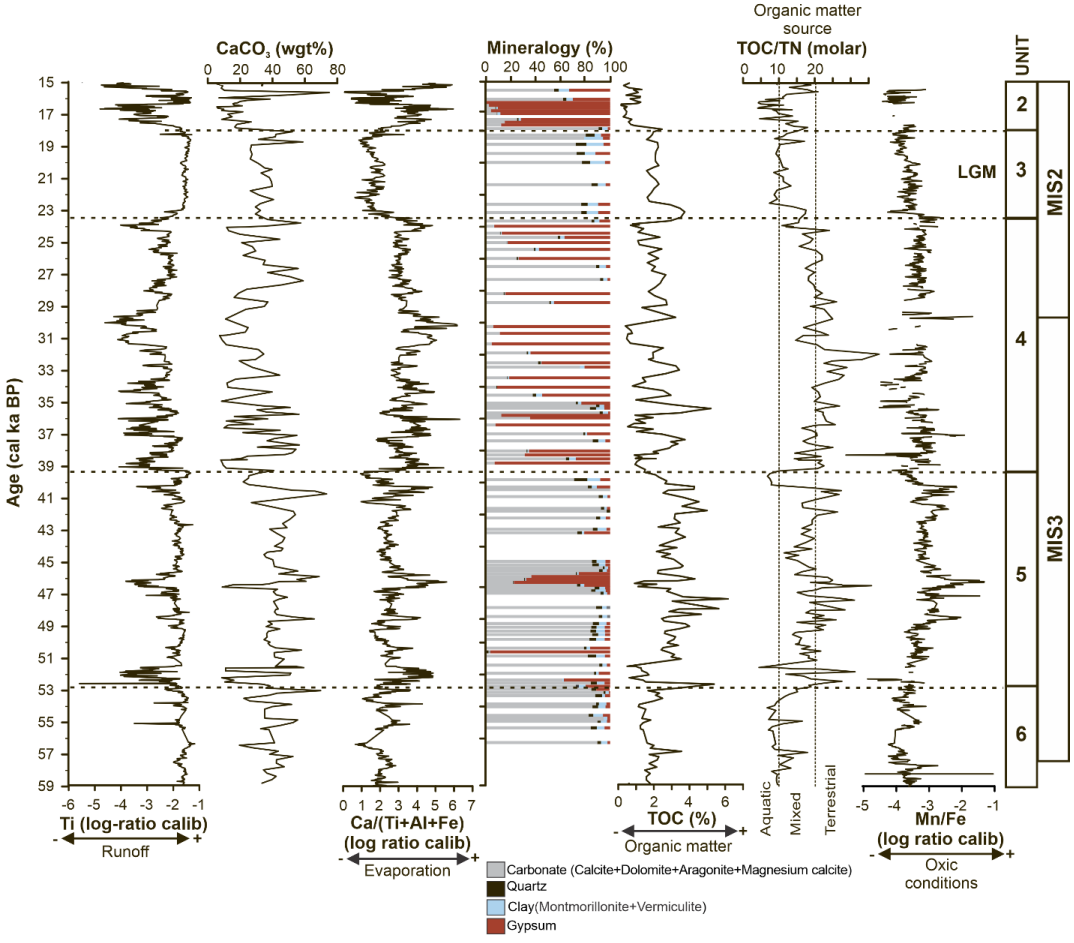

Figure 3. Comparison of proxy records of the PI-2 sequence between 59 to 15 cal ka BP. Black horizontal dotted lines indicating unit boundaries described by Mueller et al., (2010). The timing for the transitions of MIS3-2 and the Last Glacial Maximum (LGM) are shown on the right (Lisieki and Raymo, 2005). Runoff and evaporation are indicated by Ti values and Ca/Ti+Al+Fe log-ratios, respectively. CaCO3 content is shown as percentage dry weight (%wgt). Percentage of quartz, clay (montmorillonite+vermiculite) and gypsum are shown. Total organic carbon as indicator of primary productivity, Total organic carbon to total nitrogen (TOC/TN) ratios as indicators of organic matter sources, and Mn/Fe ratios as proxy for redox conditions.

https://doi.org/10.5194/egusphere-2022-787
Preprint. Discussion started: 26 August 2022

5 Discussion

Our mineralogical and geochemical analyses enabled us to define five units (Units 6-2) that correspond to the lithological classification of Mueller et al., (2010) (Table 2). Each unit corresponds to different stages in the lake evolution during MIS3 and MIS2 (59-15 cal ka BP). In the following section, we discuss the environmental and hydrological conditions that prevailed in and around Lake Petén Itzá during the deposition of each unit.

Table 2. Main lithological characteristics of Units 6 to 2 discussed in this study and previously defined by Mueller et al., (2010). We present the depth interval covering each unit, as well as the age interval calculated in this study.

Unit	Depth interval (m)	Age interval (cal ka BP)	Main lithological characteristics
2	24.7-19.0	18.0-15.0	Gypsum-rich deposits composed of massive accumulations of coarse authigenic gypsum crystals and undulating finely laminated nodular gypsum layers. Clay-rich carbonate consisting of weakly laminated calcite-montmorillonite silt.
3	29.2-24.7	23.5-18.0	Grey submillimeter-scale laminated mud rich in montmorillonite and calcite. Fragments of reworked gastropods are common.
4	44.0-29.2	39.3-23.5	Gypsum-rich composed of coarse massive brownish-yellowish gypsum sand and undulating laminated nodular gypsum layers. Clay-rich carbonate consisting of massive cream-colored silt
5	60.0-44.0	52.7-39.3	Fine laminated clayey mud rich in organic matter. The presence of up to 5 cm-thick graded turbidites is common.
6	67.0-60.0	59-52.7	Grey-laminated montmorillonite mud partly mottled with dark diffuse organic-rich spots punctuated by a graded dark turbidite sequence of silt. Fragments of reworked gastropods are common.

5.1 Hydrological and environmental conditions during MIS3-2

5.1.1 Unit 6 (59-52.7 cal ka BP): High runoff and low evaporation in the lake at the onset of MIS3

Unit 6 corresponds to the onset of MIS3. Ti is widely used as indicator for runoff (Mason and Moore 1982; Yarincik et al., 2000; Davies et al., 2015). High Ti log-ratio values (up to -1.1) in this unit suggest high runoff, particularly around 56 cal ka BP (Fig. 3). This is supported by concomitantly high clay and quartz content, with averages of 4.5 and 3.0%, respectively. Clay minerals such as montmorillonite and vermiculite are generated during chemical weathering of unstable siliciclastic minerals such as plagioclase, especially in tropical regions where atmospheric humidity is high, resulting in the enrichment of quartz (Weltje, 1994; Boggs, 2006; Van De Kamp, 2010). Lake Petén Itzá is located in a karst region (IGN, 1970). Quaternary alluvial sediments in the southeast could be the source of siliciclastic minerals (Simmons et al., 1959; Mueller, 2009). We suggest that the high clay and quartz content in Unit 6 is indicative of wetter conditions compared to the less humid environment reconstructed for the end of MIS3 (48–23

https://doi.org/10.5194/egusphere-2022-787
Preprint. Discussion started: 26 August 2022

cal ka BP) in previous studies at Site PI-6 (Hodell et al., 2008). Furthermore, the clay abundance in Unit 6 could be enhanced by the increase in precipitation and high rates of chemical weathering. This is consistent with ostracod data provided by the PI-2 record that indicate substantial precipitation in the study area during the deposition of Unit 6 (Cohuo et al., 2020).

Ca provides information on the supersaturation and precipitation of ions in solution, triggered by high evaporation (Engstrom and Wright, 1984; Boyle et al., 2001). Ca in lake sediments, however, can also originate from detrital inputs in karst regions such as the Petén as well as by authigenic formation at the lake bottom. Therefore, we normalized Ca values by indicators of detrital input such as Ti, Al and Fe, and used the Ca/Ti+Al+Fe log-ratio as an indicator of past variability in evaporation (Mason and Moore, 1982; Yarincik et al., 2000). Low Ca/Ti+Al+Fe log-ratios (mean 2.1±0.6) and gypsum content (mean 5.0±5.1%) in Unit 6 indicate low evaporation of lake water and more humid conditions, with only a few intermittent dry periods, at ~55.1 and 53.8 cal ka BP (Fig. 3). Predominantly wet conditions have also been inferred for that time in the northern Neotropics (Fig. 4) using geochemical records from Lakes Chalco (central Mexico; Martínez-Abarca et al., 2021b) and Babicora (north Mexico; Roy et al., 2013). In contrast, pollen and sedimentological information from Lake Fúquene (Colombia) indicate moderately dry conditions and a reduction in lake-surface area associated with a decline in precipitation in northern South America (Groot et al., 2013). Differences in precipitation between the northern and southern limits of the American tropics were likely associated with the latitudinal (northward) migration of the ITCZ (Fig. 5). Reflectance data from the marine sediments of the Cariaco Basin (Deplazes et al., 2013) and $\delta^{18}O$ data from marine record MD02-2529 in the Eastern Equatorial Pacific (Leduc et al., 2007) indicate a more northerly position of the ITCZ during this period.

The TOC/TN ratio has been used as an indicator for the source of organic matter in lacustrine sediment sequences (Talbot and Johannessen, 1992; Meyers and Ishiwatari, 1995). During the interval 59-53 cal ka BP, low TOC/TN ratios (mean 10.7±3.2) indicate that the sediment organic matter was predominantly of aquatic origin (Meyers et al., 2003). This is consistent with the pollen-based inference for extensive grasslands around Lake Petén Itzá, indicating that there was relatively little terrestrial biomass in the watershed that could have contributed to the lake sediments (Bush et al., 2009). The absence of arboreal vegetation, visible in the largest deposit of aquatic organic matter in our record, with the simultaneous increase in lake levels have been associated with winter rains from north cold fronts (Hodell et al., 2008). This has previously been linked to the expansion of the Laurentide Ice Sheet, bringing winter rains into Central America, producing drier summers given the high seasonality (Bradbury, 1997).

Mn/Fe ratios are used to infer variations in redox conditions in lakes (Wersin et al., 1991; Naeher et al., 2013; Friedrich et al., 2014; Ortega-Guerrero et al., 2020). Lower values of Mn/Fe generally indicate low concentration of O_2 in the water column, that is explained by a more rapid reduction of Mn than Fe under anoxic conditions favoring the preferential Mn deposition. Whereas, higher values of Mn/Fe suggest high levels of O_2, as Fe oxidizes quicker than Mn under an oxic environment. During this unit, low values of the Mn/Fe ratio (mean -3.7±0.3) in the sediments indicate anoxic conditions in the bottom waters of Lake Petén Itzá. Anoxia may have been associated with high water level as today, which prevented the wind-driven mixing of the water column.

https://doi.org/10.5194/egusphere-2022-787
Preprint. Discussion started: 26 August 2022

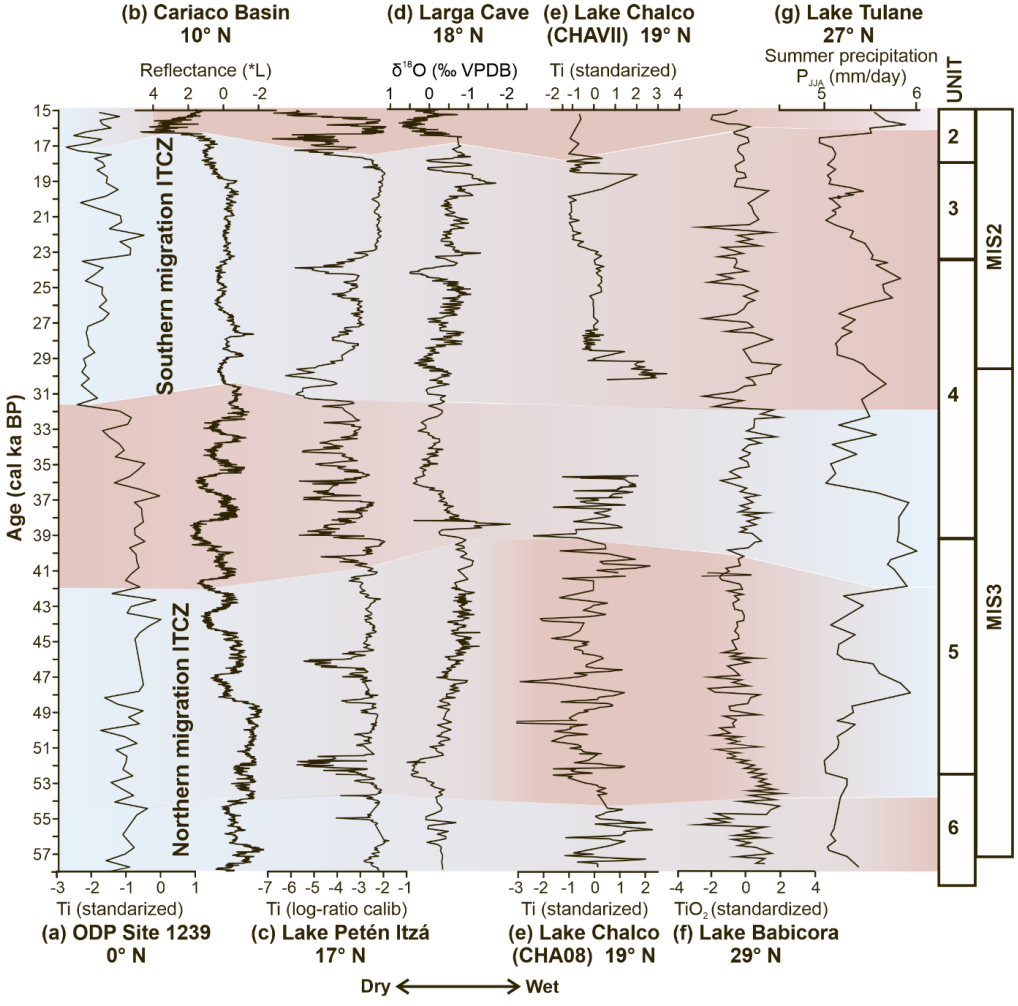

Figure 4. Comparison of paleoclimate runoff/precipitation records spanning MIS3-2. The records are arranged in latitudinal South-North order. A) Standardized record of Ti obtained from the IODP Site 1239 site in the equatorial Pacific Ocean (Rincón-Martinez et al., 2010). B) Reflectance data from the core MD03-2621 of the Cariaco Basin (Deplazes et al., 2013). C) Calibrated record of Ti from Lake Petén Itzá (This study). D) $\delta^{18}O$ data from a stalagmite from Larga Cave, Puerto Rico (Warken et al., 2020). E) Standardized record of Ti from two sedimentary sequences of Lake Chalco, Central Mexico (CHAVII site obtained from Lozano-García et al., 2015. CHA08 site from Martínez-Abarca et al., 2021b). F) Standardized TiO_2 data obtained from Lake Babicora, Northern Mexico (Roy et al., 2013). G) Numerical estimate of summer precipitation (June/July/August) made with data from Lake Tulane, Florida (Donders et al., 2011). Background colouring indicates the dominance of wet (blue) or dry (red) conditions among the records. Similarly, the preferential position of the Intertropical Convergence Zone (ITCZ) through the record is indicated. The six lithological units of the Petén Itzá record, as well as the MIS3-2 periods, are encapsulated by rectangles on the right.

https://doi.org/10.5194/egusphere-2022-787
Preprint. Discussion started: 26 August 2022

Figure 5. Map containing the different paleoclimatic records mentioned in the text as well as the limnological/climatic characteristics that are inferred for the onset of MIS3, mid-MIS3, Last Glacial Maximum (LGM) and deglaciation. The blue colors refer to mainly humid conditions while the red color indicates dry conditions. Throughout the diagrams it is possible to observe the factors that could have influenced the climatic evolution of the northern region of the Neotropics. Abbreviations: OM aqua (aquatic organic matter), OM terr (terrestrial organic matter), OM mix (mixed organic matter), Mod (moderate), SST (Superficial Sea Temperature), Carib. Curr. (Caribbean Current) .Sites: 1) Lake Babicora (Roy et al., 2013), 2) Marine record MD02-2575 (Ziegler et al., 2008), 3) Lake Tulane (Grimm et al., 2006), 4) Bahamian speleothem record AB-DC (Arienzo et al., 2017), 5) Lake Patzcuaro (Bradbury et al., 2000), 6) Lake Chalco (Martínez-Abarca et al., 2021b), 7) Lake Tecocomulco (Caballero et al., 1999), 8) Lake Petén Itzá (This study), 9) Blanchard Cave (Royer et al., 2017), 10) Larga Cave (Warken et al., 2020), 11) Marine record MD02-2529 (Leduc et al., 2007), 12) Cariaco Basin record MD03-2621 (Deplazes et al., 2013), 13) Lake Fúquene (Groot et al., 2011), 14) Marine record ODP Site 1239 (Rincón-Martínez et al., 2010).

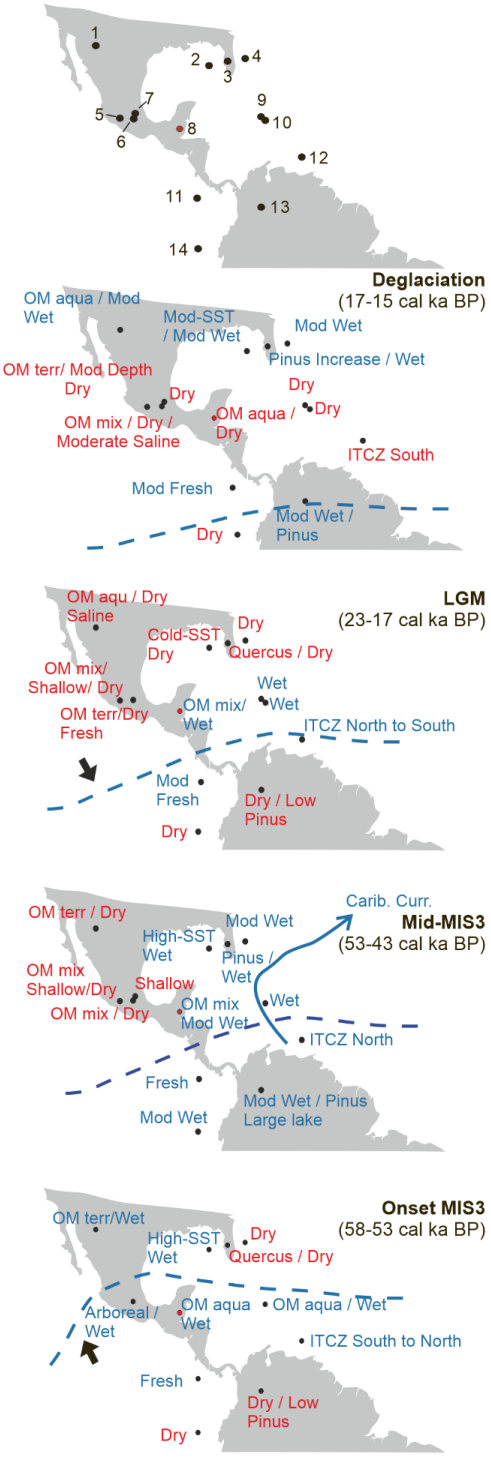

https://doi.org/10.5194/egusphere-2022-787
Preprint. Discussion started: 26 August 2022

5.1.2 Unit 5 (52.7-39.3 cal ka BP): A shift to high evaporation and low water-levels during the mid-MIS3

Ti log-ratio values (mean -2.1±0.6) indicate that precipitation and runoff to Lake Petén Itzá remained high during the deposition of Unit 5 (Fig. 3). This is also apparent from the relatively invariant quartz content (mean 3.2±2.0%), which support the inference for high precipitation and chemical weathering. Unit 5 is characterized by a pronounced increase in TOC/TN ratios (mean 18.7±5.9), indicating deposition of an admixture of aquatic and terrestrial organic matter (Meyers et al., 2003), while the increase in TOC content (mean 2.8±1.0%) indicates increased productivity and more reducing conditions in the lake. The increased relative contribution of terrestrial organic matter to the sediment is consistent with the pollen-based inference for the increase of arboreal communities such as Quercus and Pinus during Unit 5 (Correa-Metrio et al., 2012). Whereas our Petén Itzá data, together with other lake and speleothem records from the circum-Caribbean and Gulf of Mexico (e.g. Lake Tulane, Florida (Grimm et al., 2006); Abaco Island, Bahamas (Arienzo et al., 2017); Larga Cave, Puerto Rico (Warken et al., 2020) reveal moderately wet conditions, several paleoclimate records from North and Central Mexico, such as those from Lakes Babicora (Roy et al., 2013), Tecocomulco (Caballero et al., 1999), Patzcuaro (Bradbury, 2000) and Chalco (Ortega-Guerrero et al., 2020) indicate reduced rainfall at that time (Fig. 5). This climatic contrast may be associated with the position of the ITCZ over the Caribbean region and the equatorial zone. The dominance of wetter conditions in records from the Caribbean, Gulf of Mexico and Florida may suggest that moisture supply may be associated with the AMOC, since it has been shown that the strengthening of AMOC promotes an enhanced northward heat transport, a lower cross-equatorial sea-surface temperature gradient and, in consequence, wetter conditions in the tropical Northern Hemisphere (Clark et al., 2001; Waelbroeck et al., 2018). However, more modeling studies would be required to evaluate the climatic drivers consistent with data from the whole region to address this question around regional differences during the middle of MIS3.

A gradual increase in the Mn/Fe ratios suggests oxygen enrichment in the lake bottom waters during Unit 5. Particularly, two peaks of oxia are presented around 46.1 and 40.3 cal ka BP (maxima of -1.3 and -2.1 respectively; Fig. 3). Those intervals were associated with high evaporation rates, inferred from an increase in the Ca/Ti+Al+Fe ratio (up to 5.6). Our data thus suggest more oxygenated bottom waters possibly associated with a lowering of water level that resulted from greater wind-induced mixing of the water column (Yu et al., 1984; Gale et al., 2006). Increased mixing may be also associated with a reduction in the lake-surface temperature causing less stratification (e.g. Caballero and Vazquez, 2020); however, our data are not able to infer these temperature changes. These intervals of lower water level in Lake Petén Itzá were inferred previously by Pérez et al., (2021) as times of higher conductivity based on ostracod analysis. This was related to the relative increase in the concentrations of cations and anions in the water column associated with higher evaporation. In addition, the presence of the high conductivity-preferring diatom *Cyclotella petenensis* has been reported in sediments of Site PI-6 during this period (Paillès et al., 2018) and suggests a high evaporation rate. Unit 5 terminates with a short increase in runoff, as a result of more humid conditions, and aquatic organic matter input between 40.4 and 39.3 cal ka BP, as indicated by high Ti (up to -1.3) and low TOC/TN ratios (6.7).

https://doi.org/10.5194/egusphere-2022-787
Preprint. Discussion started: 26 August 2022

5.1.3 Unit 4 (39.3-23.5 cal ka BP): Great hydrological instability during the final stage of MIS3 and onset of MIS2

Unit 4 corresponds to the transition into the final stage of MIS3 and the beginning of MIS2. It is characterized by great variability in the hydrological proxies. A general and significant trend of reduced Ti content (mean -2.6±0.6) indicates a decrease in runoff. Moreover, variable but higher Ca/Ti+Al+Fe ratios (mean 3.4±0.7) indicate an increase in evaporation relative to Unit 5 (Fig. 3). In addition, $CaCO_3$ content obtained by XRD shows a similar trend to the Ti log-ratio dataset. This coupling may be response of the karstic rock composition in the catchment area. Although the entry of $CaCO_3$ into the lakes is commonly related to 1) inorganic precipitation and consequently to periods of high evaporation, and 2) high organic production that promotes eutrophication, an increase in pH and, in consequence, enhanced $CaCO_3$ (Megard, 1993; Dean, 1999), it is possible that during Unit 6 the variability of carbonate deposition in the sediments is associated with the input of detrital carbonate minerals derived from carbonate rocks in the catchment basin. Mineralogical data display higher values of gypsum (mean 53.9±34.5%), suggesting drier conditions and hence lower chemical weathering in the catchment. Stable but high contemporaneous values of Mn/Fe ratios (mean -3.3±0.4) indicates oxic bottom waters along this unit, possibly associated with a decline in water level and greater wind mixing. Lower lake levels during the MIS3-2 transition were also inferred previously in Site PI-6 by Cohuo et al., (2020) and Pérez et al., (2021) from an increase in the relative abundance of the endemic ostracod *Paracythereis opesta*, a benthic species associated with shallow-water environments (<40 m depth) (Cohuo et al., 2017; Echeverría et al., 2019). In addition, Paillès et al., (2018) found abundant diatoms belonging to *Cyclotella petenensis* and *C. cassandrae*, both characteristic for a high-conductivity environment, which agrees with our interpretation. Shallow lake level and the epilimnion establishment in the site is also supported by high $\delta^{13}C$ values measured in the ostracod *Lymnocythere opesta* at Site PI-6 (Escobar et al., 2012). Otherwise, increases in evaporation inferred from Ca/Ti+Al+Fe data simultaneous with increases in Mn/Fe ratio (bottom oxia) correlate with periods of decrease in lake volume and site exposure to the epilimnion around 37.1 and 29.6 cal ka BP. Whereas, increases in runoff at Site PI-2 correlate with an increase in lake volume and bottom anoxia at Site PI-6. Contemporaneously, contrary conditions to those present in Lake Petén Itzá have been reconstructed at lakes of central and north Mexico where wetter climate and less saline conditions prevailed (e.g. Lake Babicora, Chávez-Lara et al., 2012; Lake Chalco, Caballero et al., 2019; Fig. 4). Additionally, in more northerly records from the Gulf of Mexico, a gradual reduction in humidity is also reconstructed during the deposition of Unit 4 by paleo-precipitation models from Lake Tulane (Florida, USA) (Donders et al., 2011). This interregional comparison of paleoclimatic records indicates that the Petén Itzá region and northern Gulf of Mexico were dominated by dry conditions during the end of MIS3, however central Mexico wetter environment was established.

TOC/TN ratios rapidly increase to values >20, suggesting a relative decline in the contribution of aquatic organic matter input relative to that from terrestrial sources. After 32 cal ka BP, however, TOC/TN ratios decreased gradually to values of 10, indicating a shift to higher aquatic and lower terrestrial organic matter input. This change corresponds to an increase in sedimentary $\delta^{13}C_{TOC}$ values in the PI-6 record, which was interpreted to reflect a greater proportion of C_4 plants in the catchment area, indicative of a drier climate (Mays et al., 2017). In addition, lower TOC values (mean 1.9±1.0%) in Unit 4 suggest reduced preservation of sediment organic matter, possibly associated with higher

https://doi.org/10.5194/egusphere-2022-787
Preprint. Discussion started: 26 August 2022

oxygen concentrations at the lake bottom. The contribution of allochthonous organic matter may also have decreased because of the spread of C_4 savanna vegetation around Lake Petén Itzá, with high relative abundances of Cyperaceae and Poaceae (Correa-Metrio et al., 2012). A shift to wetter conditions occurred between 29.2 and 24.2 cal ka BP, inferred from an increase in Ti values (Fig. 3), coinciding with the start of MIS2. During that time, a reduction in the Ca/Ti+Al+Fe ratios suggest low evaporation rates, while at the same time Mn/Fe ratios remained stable.

5.1.4 Unit 3 (23.5-18.0 cal ka BP): A sudden large increase in runoff during the Last Glacial Maximum

Unit 3 corresponds to the Last Glacial Maximum (LGM), which has been studied using sediments from Site PI-6 in Lake Petén Itzá (Hodell et al., 2008; Bush et al., 2009; Pérez et al., 2011; Mays et al., 2017). Ti values are highest in Unit 3 and oscillate between -2.5 and -1.3, indicative of an abrupt increase in runoff (Fig. 3). The increase in clay and quartz contents (means of 8.5±2.9% and 5.1±2.5%, respectively) indicates an increase in humidity (Van De Kamp, 2010). Ca/Ti+Al+Fe ratios were lowest in this unit (mean -1.7±0.4), indicating significantly reduced rates of evaporation (Fig. 3). TOC/TN ratios <10 during the LGM suggest a high loading of aquatic-derived organic matter to the sediments. An average reduction in the Mn/Fe ratios (mean -3.7±0.2) and higher TOC content (2.2±0.6%) suggest that the deep lake was characterized by persistent anoxic conditions, likely associated with higher water levels. Wetter conditions and higher lake levels during the deposition of Unit 3 were also recognized in sediments of Site PI-6. High magnetic susceptibility and density values suggest high detrital input (Hodell et al., 2006, 2008), while more negative $\delta^{18}O$ and $\delta^{13}C$ values of ostracod shells indicate high lake levels and the establishment of an anoxic hypolimnion at Site PI-6 (Escobar et al., 2012; Pérez et al., 2013). Ostracod assemblage analysis revealed the presence of deep-water species (>40 m depth) such as *Cypria petenensis* (Pérez et al., 2021), while diatom data indicates low-conductivity and alkaline water during the LGM based on the presence of *Discotella gabinii* (Paillès et al., 2018). In addition, wet conditions during the LGM were inferred using oxygen stable isotope ($\delta^{18}O$) measurements in speleothems from the Caribbean region, including those from Blanchard Cave, Guadaloupe (Royer et al., 2017), Larga Cave, Puerto Rico (Warken et al., 2020), and Juxtlahuaca Cave, Guerrero, southwest Mexico (Lachniet et al., 2014). In contrast, dry conditions were deduced from other multi-proxy paleoclimate records from central and northern Mexico (e.g. La Piscina de Yuriria (Davies, 1995); Lake Patzcuaro (Bradbury, 2000); Lake Babicora (Roy et al., 2013); and Lake Chalco (Lozano-García et al., 2015)), the northern Gulf of Mexico (e.g. Lake Tulane, Florida (Grimm et al., 2006; Donders et al., 2011)), Colombia (Lake Fúquene, Groot et al., 2011, 2013; Vriend et al., 2012) and the East Equatorial Pacific ODP-1239 record (Rincón-Martínez et al., 2010) (Fig. 5). This corresponds with the Bradbury (1997) and Ramírez-Barahona and Eguiarte (2013) multi-record analyses, which showed dry conditions in western central Mexico and concomitantly wet conditions in the east. The trend observed in our regional comparison with other available records from Mexico, the Gulf of Mexico, and the Caribbean indicates that the ITCZ may have been restricted to Central America (Fig. 5). However, future numerical approach may provide more information in the reconstruction of atmospheric processes during the LGM in the Northern Neotropics.

https://doi.org/10.5194/egusphere-2022-787
Preprint. Discussion started: 26 August 2022

5.1.5 Unit 2 (18.0-15.0 cal ka BP): Low runoff and enhanced evaporation during the deglaciation

At the onset of Unit 2 (18.0-16.3 cal ka BP), a decrease in Ti values to -4.9 and increase in Ca/Ti+Al+Fe ratios and gypsum content (averages of 3.2±1.4 and 78.2±32.8%, respectively) indicate a decrease in runoff, drier conditions and an increase in evaporation rate which would have decreased the water level (Fig. 3). As Unit 4, $CaCO_3$ values are coupled with the Ti data trend in Unit 2, indicating that input of carbonates into the lake may depend on runoff and precipitation. This is consistent with ostracod-based inferences in Site PI-6 that indicate lower water levels and greater conductivity in Lake Petén Itzá with a dominance of littoral species such as *Cypridopsis vidua*, *Heterocypris putei* and *Paracythereis opesta* (Díaz et al., 2017; Cohuo et al., 2018; Pérez et al., 2021). Similarly, high $\delta^{18}O$ values of both ostracods and gypsum hydration water indicate high evaporation (Escobar et al., 2012; Hodell et al., 2012; Grauel et al., 2016). An estimated 56-m lake level decline has been reported by Anselmetti et al. (2006) and Hodell et al., (2006), based on the occurrence of a paleo shoreline in seismic images corresponding to this unit. Comparatively low TOC/TN ratios (mean 11.5±4.8) indicate a decrease in the relative contribution of organic matter from terrestrial sources. *n*-Alkane distributions in the PI-6 record show a predominance of terrestrial plant material in Unit 2 (Mays et al., 2017). Based on pollen analysis, the vegetation cover in the vicinity of the lake was largely composed of grassland (Bush et al., 2009), which probably contributed little to the sediment organic matter, as indicated by low TOC values in Unit 2 (mean 0.7±0.4%). Dry climate conditions have been deduced from lake deposits in central Mexico and the Caribbean (Bradbury 2000; Lozano-García et al., 2015; Royer et al., 2017; Caballero et al., 2019; Martínez-Abarca et al., 2019; Warken et al., 2020), whereas records from the northern Gulf of Mexico suggest wet conditions at the same time (Ziegler et al., 2008; Donders et al., 2011; Roy et al., 2013; Arienzo et al., 2017). This can be explained by the latitudinal migration to the south of the ITCZ relative to LGM caused by the AMOC collapse during HS1 that promoted dry environments throughout Central Mexico and the Caribbean (Fig. 5). It is possible that factors such as cold fronts will add moisture to the northernmost records of Mexico and the Gulf of Mexico. Unit 2 terminates with a sudden increase in Ti values (up to -1.3) between 16.3 and 15.0 cal ka BP, indicating an increase in precipitation and runoff. A decrease in Ca/Ti+Al+Fe (up to 0.1) suggests evaporation remained low, and low values of TOC/TN (up to 10.9) indicates aquatic organic matter dominated the sediment. This suggests that although dry conditions prevailed at the beginning of the deglaciation corresponding with a first stage of HS1, the second part (17-15 cal ka BP) had an increase in runoff and precipitation most likely linked to a slight AMOC recovery that precedes a second stage of HS1 in Petén Itzá (McManus et al., 2004; Hodell et al., 2012; Pérez et al. 2013).

5.2 Millennial-scale climate associated with hydrological changes in Lake Petén Itzá

Sediments from Petén Itzá Site PI-6 reveal short-term variations in lithology and in several proxies such as stable isotopes, pollen and charcoal, which have been related previously to millennial climate oscillations in Greenland and the adjacent North Atlantic, such as GI, GS and HS during MIS3-2 (Hodell et al., 2008; Correa-Metrio et al., 2012; Escobar et al., 2012). Our geochemical record from Site PI-2 supports with the association of millennial variations in Petén hydroclimate and the short-term oscillations observed in records such as the GICC05 ice core in Greenland and the marine core MD03-2621 in the Cariaco Basin, offshore Venezuela (Fig. 6). Ti data from the Petén Itzá record indicate distinct episodes of elevated runoff throughout the record, which largely correlate with the warm episodes

https://doi.org/10.5194/egusphere-2022-787
Preprint. Discussion started: 26 August 2022

GI14-2 recorded in the $\delta^{18}O$ values from the GICC05 ice core between 59 and 15 cal ka BP (Svensson et al., 2008). The presence of Ti maxima and increased clay content in Site PI-2 is largely contemporaneous with decreases in reflectance values on marine core MD03-2621, particularly within GI11-2 (Peterson et al., 2000; Deplazes et al., 2013). This indicates that the high runoff in Petén Itzá during GI was associated with the northern migration of the ITCZ inferred from the Cariaco Basin. All GI are characterized by green, clayey mud and clay-calcite silt deposits as described previously by Mueller et al., (2010) and discernible in images of the PI-2 cores (Fig. 7). The intensity of Ti maxima associated with GI11-2, and consequently the intensity of runoff, is greater in sediments older than 35 cal ka BP, suggesting that the Lake Petén Itzá basin was more susceptible to changes in precipitation and drainage during MIS3. After 35 cal ka BP, Ti maxima associated with GI are less pronounced, which may be a consequence of the more southerly average position of the ITCZ during MIS2. On the contrary, there are no clear increases in Ti values associated with the northern migration of the ITCZ during GI14-12. However, the Petén Itzá chronology has a ±2 kyr uncertainty mostly for ages >45 cal ka BP. Therefore, together with the still-discussed Greenland chronology/uncertainties for ages >42 cal ka BP (Svensson et al., 2008), we cannot exclude the possibility that the Ti increase and Ca/Ti+Al+Fe decline at 51.5, 46.8 and 45.7 cal ka BP correspond to the increments presented in the Cariaco Basin record at 53.8 (GI14), 49.3 (GI13) and 46.0 (GI12) cal ka BP, respectively.

The Ca/Ti+Al+Fe data show a series of peaks contemporaneous with decreases in Greenland $\delta^{18}O$ values associated with the cold periods of GS (Fig. 6). Hence, GS were associated with high evaporation and relatively dry conditions in Petén Itzá. Previously, Correa-Metrio et al., (2012) provided a high-resolution record of pollen and carbonized material in the Site PI-6 record (~200 year-resolution), which demonstrated an increase in forest fires in this region during GS. This is consistent with high evaporation that is in response to dry conditions in the northern Neotropics. The latter is more apparent for GS13, GS9 and GS5, whose presence in the record is synchronous with the North Atlantic IRD deposits associated with HS5-3, respectively. The enhanced Ca/Ti+Al+Fe ratios during GS13, GS9 and GS5 in Lake Petén Itzá may be a response to dry conditions that dominated during HS. In addition, higher abundances of gypsum were found during GS13 and GS9 suggesting high evaporation in the lake. Similar increases in Ca/Ti+Al+Fe ratios and gypsum content are observed during GS8, GS7, GS5, GS4 and GS3. We did not observe an increase in gypsum content during the GS11, GS10 and GS6, which is likely due to the low sampling resolution in this interval, but in which the Ca/Ti+Al+Fe ratio suggests an increase in evaporation. Samples putatively corresponding to GS14, GS12 and GS2 cannot be identified unequivocally based on the gypsum content. This may be caused by the following reasons: First, GS14 and 12 are located in a depth interval with a relatively high uncertainty of the Petén Itzá age-depth model, which makes the identification of both GS difficult. Second, GS2 is linked to the beginning of the LGM which, as discussed above, is characterized by high humidity in Petén Itzá. This likely suppressed the GS2 signal in the sediments.

https://doi.org/10.5194/egusphere-2022-787
Preprint. Discussion started: 26 August 2022

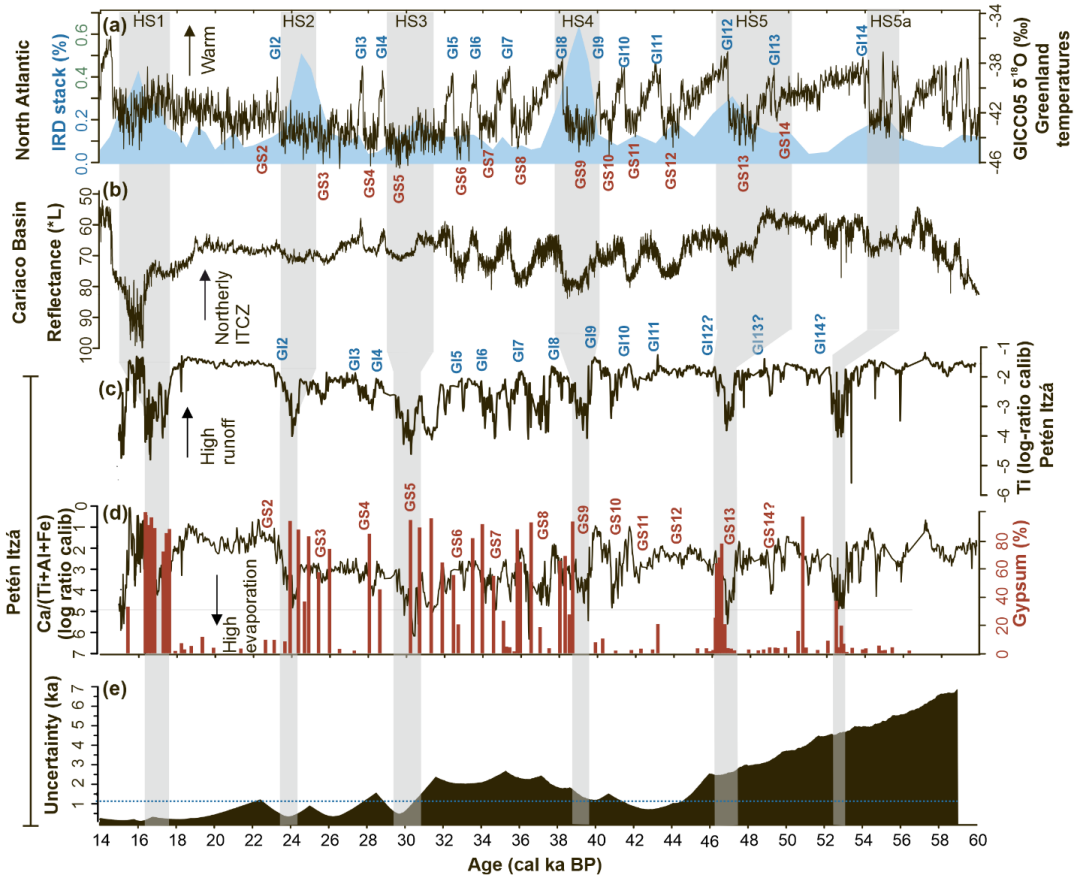

Figure 6. Temporal variation of the Petén Itzá data compared to other paleoclimatic records between 60 and 14 cal ka BP. A) North Atlantic ice rafted debris (IRD) stack derived from 15 individual sediment cores presented by Lisiecki and Stern (2016) (Blue area). Oxygen isotopes ($\delta^{18}O$) from the GICC05 (Svensson et al., 2008) ice core record in Greenland (black solid line), less negative values are warmer intervals used to define Greenland Interstadials (GI). B) Reflectance L* from the Cariaco Basin reported by Deplazes et al., (2013), lower values indicate a north migration of the Intertropical Convergence Zone (ITCZ). C) Titanium (Ti) data from the PI-2 record. D) Ca/Ti+Al+Fe ratios (black line) and gypsum data (red bars) from the PI-2 record. E) Uncertainty of the age-depth model across the PI-2 sequence. Numbers GI2-14 refer to GI. Gray shaded areas represent HS. GS recognized in the gypsum data are indicated with red labels.

https://doi.org/10.5194/egusphere-2022-787
Preprint. Discussion started: 26 August 2022

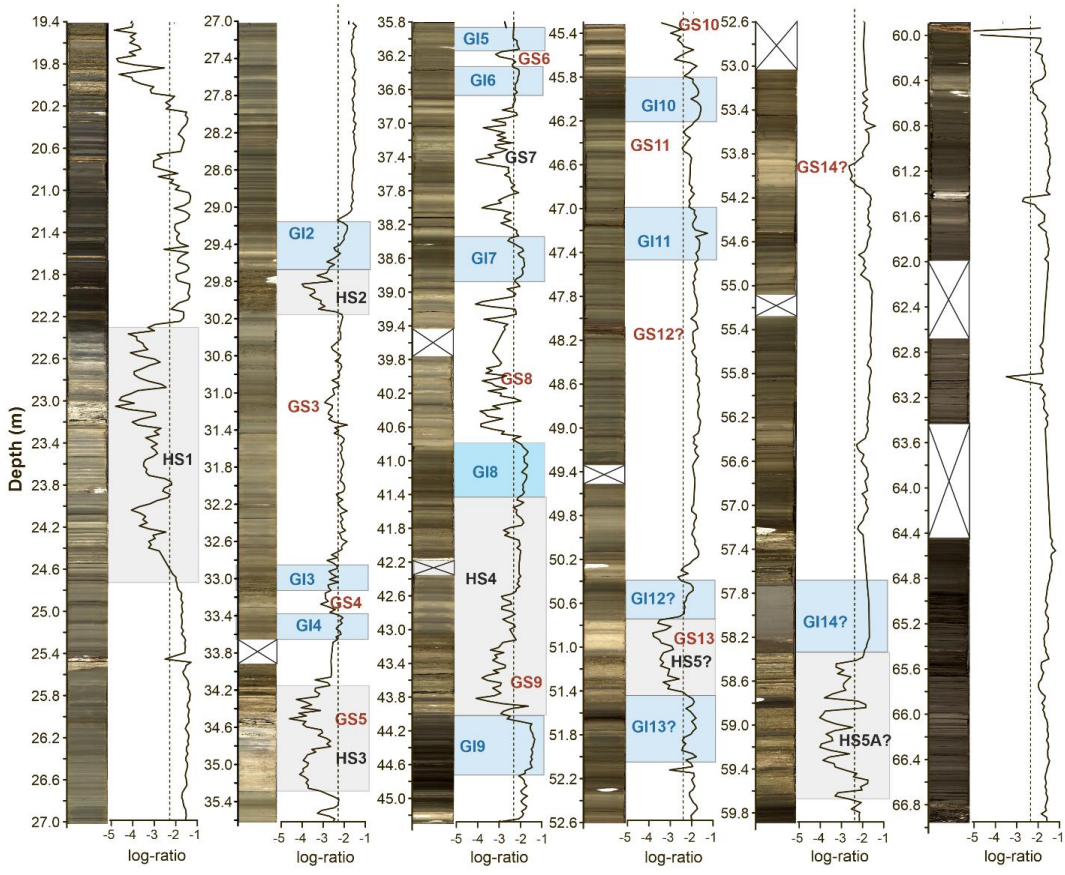

Figure 7. Composite master sequence (high-resolution sediment core photographs and Ti data) for the PI-2 record. Dotted vertical lines represent the log-ratio average Ti value of the sequence (-2.2). GI are indicated by blue bars; HS are represented by gray bars. Possible location of sediments associated with GS is indicated.

https://doi.org/10.5194/egusphere-2022-787
Preprint. Discussion started: 26 August 2022

Table 3. Chronology of Heinrich Stadials in the PI-2 record compared with glaciomarine records. The asterisk (*) refers to the beginning of each HS. Double asterisks (**) refer to the time of maximal IRD deposition. MCD = master composite depth.

	Depth site PI-2 (MCD) [m]	Age PI-2 [cal ka BP]	Age [cal ka BP] (Hemming, 2004) *	Age [cal ka BP] (Jullien et al., 2006, 2007)	Age [cal ka BP] (Hodell et al., 2010) **	Age [cal ka BP] (Lisieki and Stern, 2016) **
HS1	24.77-22.28	17.7-16.3	16.8	18.3-16.0	16.0	16.0
HS2	30.13-29.63	24.3-23.7	24.0	26.2-24	24.0	24.5
HS3	35.37-34.17	31.5-29.4	31.0	31.8-30.2	-	30.5
HS4	43.99-41.40	39.2-37.5	38.0	40.2-38.2	39.6	39.0
HS5	51.40-50.80	47.0-46.2	45.0	50.0-47.9	47.5	47.0

The new age-depth model established here shows that gypsum sand layers were deposited during the cold stages HS4-1, agreeing with previous works in Lake Petén Itzá (Hodell et al., 2008; Mueller et al., 2010; Escobar et al., 2012). Following the discussion above regarding the tuning the Petén Itzá and Cariaco Basin sequences, the recognition of HS5 would be established between GI13 and 12 (49.3-46 cal ka BP) also corresponding to the deposition of gypsum. Ages of these gypsum deposits correspond with the HS chronology presented previously for various glaciomarine records across the North Atlantic (Labeyrie et al., 1995; Hemming, 2004; Shackleton et al., 2004; Jullien et al., 2006, 2007; Hodell et al., 2010) and the compilation of several sedimentary marine records from the Atlantic, Pacific and Indian Oceans (Lisiecki and Stern, 2016; Table 3). Sediments associated with HS5-1 show Ti values below the average compared to the entire sequence (-2.2), revealing high evaporation and low runoff associated with dry conditions during their deposition. Values found in HS3 are slightly lower (-4.6) than observed in other HS, which suggests that this stage was likely characterized by driest conditions of the investigated sequence.

Our inferences are similar to the reconstructed record from Site PI-6, confirming that the lake response to hydroclimate change was the same among sites in the lake. Ostracod data, for example, suggest that HS3-1 were characterized by high lake-water conductivity, associated with an increase in evaporation and a reduction in runoff (Pérez et al., 2021). In addition, pollen records show the establishment of savanna vegetation associated with dry conditions and a drop-in mean annual air temperature of up to 6°C (Correa-Metrio et al., 2012; Hodell et al., 2012). Moreover, $\delta^{13}C$ and $\delta^{18}O$ values in ostracods indicate a lowering of lake level such that Site PI-6 was within the oxygen-rich epilimnion (Escobar et al., 2012). This agrees with paleoclimate records from the Eastern Equatorial Pacific, the Caribbean and Central Mexico (Leduc et al., 2007; Arienzo et al., 2015, 2017; Medina-Elizalde et al., 2017; Hodell et al., 2017; Caballero et al., 2019), which suggests that HS4-1 were generally dry and cold. The dry response in Lake Petén Itzá during the HS correlates with the worldwide recognized "Tropical Hydroclimatic Events (THEs)", in which extreme regional anomalies in rainfall occurred (Bradley and Díaz, 2020). The dominance of dry conditions in the Caribbean region during THEs was favored by meltwater input to the North Atlantic that, in turn, reduced the Atlantic Meridional Oceanic Circulation. As a result, the mean position of the ITCZ moved approximately 1° to the south, promoting droughts not only in the northern Neotropics but also in Africa and the Arabian Peninsula (Tjallingii et al., 2008; Zarreiss et al., 2011).

https://doi.org/10.5194/egusphere-2022-787
Preprint. Discussion started: 26 August 2022

6 Conclusions

Using the sediment record from Site PI-2 in Lake Petén Itzá, we inferred changes in runoff, evaporation intensity, organic matter provenance and redox conditions during MIS3-2 (59-15 cal ka BP). MIS3 was a period of high variability in Lake Petén Itzá with large changes in runoff and evaporation on millennial time scales. The end of MIS3 (39.3-29 cal ka BP), however, was characterized by a gradual decline in runoff and increase in evaporation. This shift was accompanied by input of mixed aquatic and terrestrial organic matter and more oxygenated bottom waters, perhaps related to low water levels near the end of MIS3. MIS2 was a dry period with low runoff, with the exception of the Last Glacial Maximum, when wet conditions prevailed. During the LGM, lake sediments received relatively greater contributions of aquatic organic matter, and hypolimnetic waters were persistently anoxic, presumably associated with deep-water conditions. Comparison of our record with regional data from the northern Neotropics, the Caribbean, Florida, and northern Mexico indicate that variability in runoff and consequently precipitation in the region during MIS3-2 was influenced by the latitudinal migration of the ITCZ in response to changes in the strength of the AMOC. Millennial climate events such as GI14-2, GS14-2 and HS5-1 were identified in the PI-2 record and show similar responses to those reconstructed for Site PI-6. HS and GS were marked by high evaporation in Lake Petén Itzá associated with dry conditions. In particular, GS13, 9 and 5 showed dry conditions as they were contemporaneous to HS5 to 3, respectively. Moreover, GIs were associated with high runoff and low evaporation in the lake linked to the dominance of wet conditions in the region. Overall, GIs in Petén Itzá were marked by relatively wet environments, with high runoff and precipitation in sediments older than 35 kyr possibly linked to a persistent northern position of the ITCZ. The Petén Itzá sediments offer one of the few records from the northern edge of the Neotropics that has adequate resolution for the identification and future studies of millennial climate oscillations.

Author contribution

All of the authors listed made substantial contributions to the manuscript and qualify for authorship. DH, MB, JC, DA, and FA led the Petén Itzá Scientific Drilling Project that collected and described the cores and obtained the material for radiocarbon dating that was done by TG. RMA, AS, LP and TB directed the research and participated in drafting the manuscript; MA, PH, DH and SK reviewed the data; MB, DH, SC, LMG, MS, JC, FA, DA, TG, ACM and FS reviewed the manuscript critically. We acknowledge that all the authors have agreed to this submission.

Competing interests:

The authors declare that they have no conflict of interest.

Acknowledgments

We thank all our colleagues and the institutions involved in the Petén Itzá Drilling Project. In particular, we thank Andreas Mueller, Jaime Escobar, Adrian Gilli, Florence Sylvestre, Dominik Schmidt, Esmeralda Cruz, Mark Bush, as well as Kristina Brady, Anders Noren and other colleagues from the National Lacustrine Core Repository (LacCore, University of Minnesota) for their participation and for organizing and providing data. We especially thank Jonathan Obrist-Farner, Rik Tjallingii and Robert Brown for helping during calibration analyses. Funding was provided by the Deutsche Forschungsgemeinschaft (DFG grants 5448462, 235297191, 252760755, 439719305, KU2685/3-1 and

https://doi.org/10.5194/egusphere-2022-787
Preprint. Discussion started: 26 August 2022

SCHW671/16-1), Technische Universitat Braunschweig, US National Science Foundation (ATM-0502030), Swiss National Science Foundation (grant 620-066113), the Swedish Research Council for Sustainable Development (FORMAS grant 2020-01000) and the International Continental Scientific Drilling Program.

References

Anselmetti, F. S., Ariztegui, D., Hodell, D. A., Hillesheim, M. B., Brenner, M., Gilli, A., McKenzie, J.A., and Mueller, A. D.: Late Quaternary climate-induced lake level variations in Lake Petén Itzá, Guatemala, inferred from seismic stratigraphic analysis, Palaeogeogr. Palaeoclimatol. Palaeoecol., 230 (1-2), 52-69, https://doi.org/10.1016/j.palaeo.2005.06.037, 2006.

Arienzo, M.M., Swart, P.K., Pourmand, A., Broad, K., Clement, A.C., Murphy, L.N., Vonhof, H.B., and Kakuk, B.: Bahamas speleothem reveals climate variability associated with Heinrich events. Earth Planet. Sci. Lett. 430, 377-386, https://doi.org/10.1016/j.epsl.2015.08.035, 2015.

Arienzo, M. M., Swart, P. K., Broad, K., Clement, A. C., Pourmand, A., and Kakuk, B.: Multi-proxy evidence of millennial climate variability from multiple Bahamian speleothems, Quat. Sci. Rev., 161, 18-29, https://doi.org/10.1016/j.quascirev.2017.02.004, 2017.

Blaauw, M: Out of tune: the dangers of aligning proxy archives, Quat. Sci. Rev., 36, 38-49, https://doi.org/10.1016/j.quascirev.2010.11.012, 2012.

Blaauw, M., and Christen, J. A.: Flexible paleoclimate age-depth models using an autoregressive gamma process, Bayesian Anal., 6(3), 457-474, https://doi.org/10.1214/11-BA618, 2011.

Bloemsma, M. R.: Development of a modelling framework for core data integration using XRF scanning, Ph.D. thesis, Delft University of Technology, Netherlands, 229 pp., 2015.

Bradbury, J. P.: Sources of glacial moisture in Mesoamerica, Quat. Int., 43, 97-110, https://doi.org/10.1016/S1040-6182(97)00025-6, 1997.

Bradbury, J. P.: Limnologic history of Lago de Patzcuaro, Michoacan, Mexico for the past 48,000 years: impacts of climate and man, Palaeogeogr. Palaeoclimatol. Palaeoecol., 163(1-2), 69-95, https://doi.org/10.1016/S0031-0182(00)00146-2, 2000.

Bradley, R. S., and Diaz, H. F.: Late Quaternary abrupt climate change in the tropics and sub-tropics: The continental signal of Tropical Hydroclimatic Events (THEs), Rev. Geophys., 59 (4), https://doi.org/10.1029/2020RG000732, 2021.

Broecker, W., Bond, G., Klas, M., Clark, E., and McManus, J.: Origin of the northern Atlantic's Heinrich events, Climate Dynamics, 6(3), 265-273, https://doi.org/10.1007/BF00193540, 1992.

Boggs, S. (Ed.): Principles of sedimentology and stratigraphy, Pearson Prentice Hall, New Jersey, USA, 2006.

https://doi.org/10.5194/egusphere-2022-787
Preprint. Discussion started: 26 August 2022

Boyle, J. F.: Organic geochemical methods in palaeolimnology, in: Tracking environmental change using lake sediments, edited by: Last, W., and Smol, J.P., Springer, Dordrecht, The Netherlands, 83-141, 2001.

Burns, S. J., Fleitmann, D., Matter, A., Neff, U., and Mangini, A.: Speleothem evidence from Oman for continental pluvial events during interglacial periods, Geology, 29(7), 623-626, https://doi.org/10.1130/0091-7613(2001)029%3C0623:SEFOFC%3E2.0.CO;2, 2001.

Bush, M. B., Correa-Metrio, A. Y., Hodell, D. A., Brenner, M., Anselmetti, F. S., Ariztegui, D., Mueller, A.D., Curtis, J.H., Grzesik, D.A., Burton, C., and Gilli, A.: Re-evaluation of climate change in lowland Central America during the Last Glacial Maximum using new sediment cores from Lake Petén Itzá, Guatemala, in: Past climate variability in South America and surrounding regions, edited by: Vimeux, F., Sylvestre, F., Khodri, M., Springer, Dordrecht, The Netherlands, 113-128, https://doi.org/10.1007/978-90-481-2672-9_5, 2009.

Caballero, M., and Vázquez, G.: Mixing patterns and deep chlorophyll a maxima in an eutrophic tropical lake in western Mexico, Hydrobiologia, 847(20), 4161-4176, https://doi.org/10.1007/s10750-020-04367-y, 2020.

Caballero, M., Lozano, S., Ortega, B., Urrutia, J., and Macias, J. L.: Environmental characteristics of Lake Tecocomulco, northern basin of Mexico, for the last 50,000 years, J Paleolimnol., 22(4), 399-411, https://doi.org/10.1023/A:1008012813412, 1999.

Caballero, M., Lozano-García, S., Ortega-Guerrero, B., and Correa-Metrio, A.: Quantitative estimates of orbital and millennial scale climatic variability in central Mexico during the last~ 40,000 years, Quat. Sci. Rev., 205, 62-75, https://doi.org/10.1016/j.quascirev.2018.12.002, 2019.

Chávez-Lara, C. M., Roy, P. D., Caballero, M. M., Carreño, A. L., and Lakshumanan, C.: Lacustrine ostracodes from the Chihuahuan Desert of Mexico and inferred Late Quaternary paleoecological conditions, Rev. Mex. de Cienc. Geol., 29(2), 422-431, http://www.scielo.org.mx/scielo.php?script=sci_arttext&pid=S1026-87742012000200010&lng=es&nrm=iso, 2012.

Clark, P. U., Marshall, S. J., Clarke, G. K., Hostetler, S. W., Licciardi, J. M., and Teller, J. T.: Freshwater forcing of abrupt climate change during the last glaciation, Science, 293(5528), 283-287, https://doi.org/10.1126/science.1062517, 2001.

Cohuo, S., Macario-González, L., Pérez, L., and Schwalb, A.: Overview of Neotropical-Caribbean freshwater ostracode fauna (Crustacea, Ostracoda): identifying areas of endemism and assessing biogeographical affinities, Hydrobiologia, 1-17, https://doi.org/10.1007/s10750-016-2747-1, 2017.

Cohuo, S., Macario-González, L., Pérez, L., Sylvestre, F., Paillès, C., Curtis, J. H., Kuterolf, S., Wojewódka, M., Zawisza, E., Szeroczynska, K., and Schwalb, A.: Climate ultrastructure and aquatic community response to Heinrich Stadials (HS5a-HS1) in the continental northern Neotropics, Quat. Sci. Rev., 197, 75-91, https://doi.org/10.1016/j.quascirev.2018.07.015, 2018.

https://doi.org/10.5194/egusphere-2022-787
Preprint. Discussion started: 26 August 2022

Cohuo, S., Macario-González, L., Wagner, S., Naumann, K., Echeverría-Galindo, P., Pérez, L., Curtis, J., Brenner, M., and Schwalb, A: Influence of late Quaternary climate on the biogeography of Neotropical aquatic species as reflected by non-marine ostracodes. Biogeosciences, 17(1), 145-161, https://doi.org/10.5194/bg-17-145-2020, 2020.

Correa-Metrio, A., Bush, M. B., Cabrera, K. R., Sully, S., Brenner, M., Hodell, D. A., Escobar, J., and Guilderson, T.: Rapid climate change and no-analog vegetation in lowland Central America during the last 86,000 years. Quat. Sci. Rev., 38, 63-75, https://doi.org/10.1016/j.quascirev.2012.01.025, 2012.

Dansgaard, W., Johnsen, S. J., Clausen, H. B., Dahl-Jensen, D., Gundestrup, N. S., Hammer, C. U., Hvidberg, C.S., Steffensen, J.P. Sveinbjörnsdottir, A.E. Jozuel, J., and Bond, G.: Evidence for general instability of past climate from a 250-kyr ice-core record, Nature, 364(6434), 218-220, https://doi.org/10.1038/364218a0, 1993.

Davies, H.: Quaternary Palaeolimnology of a Mexican Crater Lake. Ph.D. thesis, University of Kingston, United Kingdom, 248 pp., 1995.

Davies, S., Lamb, H., and Roberts, S.: Micro-XRF Core Scanning in Palaeolimnology: Recent Developments, in: Micro-XRF Studies of Sediment Cores. Developments in Paleoenvironmental Research Vol.17, edited by: Croudace, I., and Rothwell, R., Springer, Dordrecht. The Netherlands, 189-226, https://doi.org/10.1007/978-94-017-9849-5_7, 2015.

Dean, W. E.: The carbon cycle and biogeochemical dynamics in lake sediments, J Paleolimnol, 21(4), 375-393, https://doi.org/10.1023/A:1008066118210, 1999.

Deplazes, G., Lückge, A., Peterson, L. C., Timmermann, A., Hamann, Y., Hughen, K. A., Röhl, U., Laj, C., Cane, M.A., Sigman D.M. and Haug, G. H.: Links between tropical rainfall and North Atlantic climate during the last glacial period. Nat. Geosci., 6(3), 213-217, https://doi.org/10.1038/ngeo1712, 2013.

Díaz, K.A., Pérez, L., Correa-Metrio, A., Franco-Gaviria, J.F., Echeverría, P., Curtis, J., and Brenner, M.: Holocene environmental history of tropical, mid-altitude Lake Ocotalito, México, inferred from ostracodes and non-biological indicators, The Holocene, 27(9), 1308-1317, https://doi.org/10.1177%2F0959683616687384, 2017.

Donders, T. H., de Boer, H. J., Finsinger, W., Grimm, E. C., Dekker, S. C., Reichart, G. J., and Wagner-Cremer, F.: Impact of the Atlantic Warm Pool on precipitation and temperature in Florida during North Atlantic cold spells, Climate Dynamics, 36(1-2), 109-118, https://doi.org/10.1007/s00382-009-0702-9, 2011.

Dunlea, A. G., Murray, R. W., Tada, R., Alvarez-Zarikian, C. A., Anderson, C. H., Gilli, A., Giosan, L., Gorgas, T., Hennekam, R., Irino T., Murayama, M., Peterson, L., Reichart, G.J. Seki, A., Zheng, H., and Ziegler, M.: Intercomparison of XRF core scanning results from seven labs and approaches to practical calibration, Geochemistry, Geophys. Geosystems, 21(9), https://doi.org/10.1029/2020GC009248, 2020.

Echeverría Galindo, P. G., Pérez, L., Correa-Metrio, A., Avendaño, C. E., Moguel, B., Brenner, M., Cohuo, S., Macario, L., Caballero, M., and Schwalb, A.: Tropical freshwater ostracodes as environmental indicators across an

https://doi.org/10.5194/egusphere-2022-787
Preprint. Discussion started: 26 August 2022

altitude gradient in Guatemala and Mexico, Rev. Biol. Trop., 67(4), 1037-1058. https://doi.org/10.15517/RBT.V67I4.33278, 2019.

Engleman, E. E., Jackson, L. L., and Norton, D. R.: Determination of carbonate carbon in geological materials by coulometric titration, Chem. Geol., 53(1-2), 125-128, 1985

Engstrom, D. R., and Wright Jr, H. E.: Chemical stratigraphy of lake sediments as a record of environmental change, in: Lake sediments and environmental history: studies in palaeolimnology and palaeoecology in honour of Winifred Tutin, edited by: Haworth, E.Y. and Lund, J.W.G., Leicester University Press, United Kingdom, 1984.

Escobar, J., Hodell, D. A., Brenner, M., Curtis, J. H., Gilli, A., Mueller, A. D., Anselmetti F.S. Ariztegui D., Grzesik D.A., Pérez, L., Schwalb A., and Guilderson, T. P.: A~ 43-ka record of paleoenvironmental change in the Central American lowlands inferred from stable isotopes of lacustrine ostracods, Quat. Sci. Rev., 37, 92-104, https://doi.org/10.1016/j.quascirev.2012.01.020, 2012.

Friedrich, J., Janssen, F., Aleynik, D., Bange, H. W., Boltacheva, N., Çagatay, M. N., Dale, A.W., et al.: Investigating hypoxia in aquatic environments: diverse approaches to addressing a complex phenomenon, Biogeosciences, 11(4), 1215-1259, https://doi.org/10.5194/bg-11-1215-2014, 2014.

Gale, E., Pattiaratchi, C., and Ranasinghe, R.: Vertical mixing processes in intermittently closed and open lakes and lagoons, and the dissolved oxygen response, Estuar. Coast. Shelf Sci., 69(1-2), 205-216, https://doi.org/10.1016/j.ecss.2006.04.013, 2006

Grimm, E. C., Watts, W. A., Jacobson Jr, G. L., Hansen, B. C., Almquist, H. R., and Dieffenbacher-Krall, A. C.: Evidence for warm wet Heinrich events in Florida, Quat. Sci. Rev., 25(17-18), 2197-2211, https://doi.org/10.1016/j.quascirev.2006.04.008, 2006.

Grauel, A.-L., Hodell, D.A., and Bernasconi, S.M.: Quantitative estimates of tropical temperature change in lowland Central America during the last 42 ka, Earth Planet. Sci. Lett., 438, 37–46, https://doi.org/10.1016/j.epsl.2016.01.001, 2016.

Groot, M. H. M., Lourens, L. J., Hooghiemstra, H., Vriend, M., Berrio, J. C., Tuenter, E., Van der Plicht, J., Van Geel, B., Ziegler, M., Weber, S. L., Betancourt, A., et al.: Ultra-high resolution pollen record from the northern Andes reveals rapid shifts in montane climates within the last two glacial cycles, Clim. Past, 7(1), 299-316, https://doi.org/10.5194/cp-7-299-2011, 2011.

Groot, M. H., Hooghiemstra, H., Berrio, J. C., and Giraldo, C.: North Andean environmental and climatic change at orbital to submillennial time-scales: vegetation, water levels and sedimentary regimes from Lake Fúquene 130–27 ka. Rev. Palaeobot. Palynol., 197, 186-204, https://doi.org/10.1016/j.revpalbo.2013.04.005, 2013.

Heinrich, H.: Origin and consequences of cyclic ice rafting in the Northeast Atlantic Ocean during the past 130,000 years, Quat. Res., 29, 143–152, https://doi.org/10.1016/0033-5894(88)90057-9, 1988.

https://doi.org/10.5194/egusphere-2022-787
Preprint. Discussion started: 26 August 2022

Hemming, S. R.: Heinrich events: Massive late Pleistocene detritus layers of the North Atlantic and their global climate imprint, Rev. Geophys., 42(1), https://doi.org/10.1029/2003RG000128, 2004.

Hodell, D., Anselmetti, F., Brenner, M., and Ariztegui, D.: The Lake Petén Itzá Scientific Drilling Project, Sci. Drill., 3, 25-29, https://doi.org/10.2204/iodp.sd.3.02.2006, 2006.

Hodell, D. A., Anselmetti, F. S., Ariztegui, D., Brenner, M., Curtis, J. H., Gilli, A., Grzesik, D.A., Guilderson, T.J., Mueller A. D., Bush, M.B., Correa-Metrio, A., Escobar, J., and Kutterolf, S.: An 85-ka record of climate change in lowland Central America. Quat. Sci. Rev., 27(11-12), 1152-1165, https://doi.org/10.1016/j.quascirev.2008.02.008, 2008.

Hodell, D. A., Evans, H. F., Channell, J. E., and Curtis, J. H.: Phase relationships of North Atlantic ice-rafted debris and surface-deep climate proxies during the last glacial period, Quat. Sci. Rev., 29(27-28), 3875-3886., https://doi.org/10.1016/j.quascirev.2010.09.006, 2010.

Hodell, D.A., Turchyn, A.V., Wiseman, C.J., Escobar, J., Curtis, J.H., Brenner, M., Gilli, A., Mueller, A.D., Anselmetti, F., Ariztegui, D., and Brown, E.T.: Late Glacial temperature and precipitation changes in the lowland Neotropics by tandem measurements of δ18O in biogenic carbonate and gypsum hydration water, Geochim. Cosmochim. Acta 77, 352–368, https://doi.org/10.1016/j.gca.2011.11.026, 2012.

Hodell, D. A., Nicholl, J. A., Bontognali, T. R., Danino, S., Dorador, J., Dowdeswell, J. A., Einsle, J., Kuhlmann H., Martrat, B., Mleneck-Vautravers, M.J., Rodríguez-Tovar, F.J., and Röhl, U.: Anatomy of Heinrich Layer 1 and its role in the last deglaciation, Paleoceanography, 32(3), 284-303, https://doi.org/10.1002/2016PA003028, 2017

Instituto Geográfico Nacional – IGN (1970) Carta Geológica de la Republica de Guatemala. Esc: 1:500,000.

Instituto Nacional de Sismología, Vulcanología, Meteorología e Hidrología - INSIVUMEH (2021) Información meteorológica. Access by: https:// tps://gae.insivumeh.gob.gt/publico

Jullien, E., Grousset, F. E., Hemming, S. R., Peck, V. L., Hall, I. R., Jeantet, C., and Billy, I.: Contrasting conditions preceding MIS3 and MIS2 Heinrich events, Glob Planet Change, 54(3-4), 225-238, https://doi.org/10.1016/j.gloplacha.2006.06.021, 2006.

Jullien, E., Grousset, F., Malaizé, B., Duprat, J., Sanchez-Goni, M. F., Eynaud, F., Charlier, K., Schneider, R., Bory, A., Bout, B., and Flores, J. A.: Low-latitude "dusty events" vs. high-latitude "icy Heinrich events, Quat. Res., 68(3), 379-386, https://doi.org/10.1016/j.yqres.2007.07.007, 2007.

Kylander, M. E., Ampel, L., Wohlfarth, B., and Veres, D.: High-resolution X-ray fluorescence core scanning analysis of Les Echets (France) sedimentary sequence: new insights from chemical proxies. J Quat Sci, 26(1), 109-117, https://doi.org/10.1002/jqs.1438, 2011.

Kutterolf, S., Schindlbeck, J. C., Anselmetti, F. S., Ariztegui, D., Brenner, M., Curtis, J., Schmid, D., Hodell, D.A., Mueller, A, Pérez, L., Pérez, W., Schwalb, A., Frische, M., and Wang, K.L.: A 400-ka tephrochronological framework

https://doi.org/10.5194/egusphere-2022-787
Preprint. Discussion started: 26 August 2022

for Central America from Lake Petén Itzá (Guatemala) sediments, Quat. Sci. Rev., 150, 200-220, https://doi.org/10.1016/j.quascirev.2016.08.023, 2016.

Labeyrie, L., Vidal, L., Cortijo, E., Paterne, M., Arnold, M., Duplessy, J.C., Vautravers, M.L., Labracherie, M., Duprat, J., Turon, J.L., Grousset, F.E., and van Weering, T.: Surface and deep hydrology of the northern Atlantic Ocean during the past 150,000 years, Philosophical Transactions of the Royal Society of London, 348, 255–264, https://doi.org/10.1098/rstb.1995.0067, 1995.

Lachniet, M. S., Denniston, R. F., Asmerom, Y., and Polyak, V. J.: Orbital control of western North America atmospheric circulation and climate over two glacial cycles. Nat. Commun., 5(1), 1-8., https://doi.org/10.1038/ncomms4805, 2014.

Last, W. M.: Mineralogical analysis of lake sediments, in: Tracking environmental change using lake sediments, edited by: Last, W., and Smol, J.P., Springer, Dordrecht, The Netherlands, 143-187, 2001.

Leduc, G., Vidal, L., Tachikawa, K., Rostek, F., Sonzogni, C., Beaufort, L., and Bard, E.: Moisture transport across Central America as a positive feedback on abrupt climatic changes, Nature, 445(7130), 908-911, https://doi.org/10.1038/nature05578, 2007.

Lisiecki, L. E., and Raymo, M. E.: A Pliocene-Pleistocene stack of 57 globally distributed benthic δ18O records, Paleoceanography, 20(1), https://doi.org/10.1029/2004PA001071, 2005.

Lisiecki, L. E., and Stern, J. V.: Regional and global benthic δ18O stacks for the last glacial cycle, Paleoceanogr Paleoclimatol, 31(10), 1368-1394, https://doi.org/10.1002/2016PA003002, 2016.

Lozano-García, S., Ortega, B., Roy, P. D., Beramendi-Orosco, L., and Caballero, M.: Climatic variability in the northern sector of the American tropics since the latest MIS 3, Quat Res., 84(2), 262-271, https://doi.org/10.1016/j.yqres.2015.07.002, 2015.

Marshall, M. H., Lamb, H. F., Huws, D., Davies, S. J., Bates, R., Bloemendal, J., Boyle, J., Leng, M.J., Umer, M. and Bryant, C.: Late Pleistocene and Holocene drought events at Lake Tana, the source of the Blue Nile, Glob Planet Change, 78(3-4), 147-161, https://doi.org/10.1016/j.gloplacha.2011.06.004, 2011.

Martínez-Abarca, R., Lozano-García, S., Ortega-Guerrero, B., and Caballero-Miranda, M.: Incendios y actividad volcánica: historia de fuego en la cuenca de México en el Pleistoceno tardío con base en registros de material carbonizado en el lago de Chalco, Rev. Mex. de Cienc. Geol., 36(2), 259-269, https://www.redalyc.org/articulo.oa?id=57265251009, 2019.

Martínez-Abarca, R., Ortega-Guerrero, B., Lozano-García, S., Caballero, M., Valero-Garcés, B., McGee, D., Brown, E.T., Stockhecke, M., and Hodgetts, A. G.: Sedimentary stratigraphy of Lake Chalco (Central Mexico) during its formative stages, Int J Earth Sci., 110(7), 2519-2539, https://doi.org/10.1007/s00531-020-01964-z, 2021a

Martínez-Abarca, L. R., Lozano-García, S., Ortega-Guerrero, B., Chávez-Lara, C. M., Torres-Rodríguez, E., Caballero, M., Brown, E.T, Sosa-Najera, S., Acosta-Noriega, C., and Sandoval-Ibarra, V.: Environmental changes

https://doi.org/10.5194/egusphere-2022-787
Preprint. Discussion started: 26 August 2022

during MIS6-3 in the Basin of Mexico: A record of fire, lake productivity history and vegetation, J South Am Earth Sci., 109, 103231, https://doi.org/10.1016/j.jsames.2021.103231, 2021b

Mason, B., and Moore, C. B. (Eds.): Principles of geochemistry (4th Edition), John Wiley & Sons, New York, USA, 1982.

Mays, J. L., Brenner, M., Curtis, J. H., Curtis, K. V., Hodell, D. A., Correa-Metrio, A., Escobar, J., Dutton, A.L., Zimmerman A. R., and Guilderson, T. P.: Stable carbon isotopes (δ 13 C) of total organic carbon and long-chain n-alkanes as proxies for climate and environmental change in a sediment core from Lake Petén-Itzá, Guatemala, J Paleolimnol, 57(4), 307-319, https://doi.org/10.1007/s10933-017-9949-z, 2017

McManus, J., Francois, R., Gherardi, J.M., Keigwin, L.D., and Brown-Leger, S.: Collapse and rapid resumption of Atlantic meridional circulation linked to deglacial climate changes, Nature, 428, 834–837, https://doi.org/10.1038/nature02494, 2004.

Medina-Elizalde, M., Burns, S. J., Polanco-Martinez, J., Lases-Hernández, F., Bradley, R., Wang, H. C., and Shen, C. C.: Synchronous precipitation reduction in the American Tropics associated with Heinrich 2, Sci. Rep., 7(1), 1-12, https://doi.org/10.1038/s41598-017-11742-8, 2017

Megard, R. O.: Environment of deposition of CaCO3 in Elk lake, Minnesota, in: Elk Lake, Minnesota: Evidence for rapid climate change in the north-central United States, edited by: Bradbury, J.P., and Dean, E., U.S. Geological Survey, Colorado, USA, 97-115, 1993.

Mestas-Nunez, A.M., Enfield, D.B., and Zhang, C.: Water vapor fluxes over the Intra-Americas Sea: seasonal and interannual variability and associations with rainfall, J. Clim., 20 (9), 1910–1922, https://doi.org/10.1175/JCLI4096.1, 2007.

Meyers, P. A.: Applications of organic geochemistry to paleolimnological reconstructions: a summary of examples from the Laurentian Great Lakes, Org. Geochem., 34(2), 261-289, https://doi.org/10.1016/S0146-6380(02)00168-7, 2003.

Meyers, P. A., and Ishiwatari, R.: Organic matter accumulation records in lake sediments, in: Physics and chemistry of lakes, edited by: Lerman, A., Imboden, D.M. and Ga, J.R., Springer, Berlin, Germany, 279-328, 1995.

Moernaut, J., Van Daele, M., Strasser, M., Clare, M. A., Heirman, K., Viel, M., Cardenas, J., Kilian, R., Ladron de Guevara, B., Pino, M., Urrutia, R., and De Batist, M.: Lacustrine turbidites produced by surficial slope sediment remobilization: a mechanism for continuous and sensitive turbidite paleoseismic records, Mar. Geol., 384, 159-176, https://doi.org/10.1016/j.margeo.2015.10.009, 2017.

Mueller, A. D.: Late Quaternary Environmental Change in the Lowland Neotropics: The Petén Itzá Scientific Drilling Project, Guatemala, Ph.D. thesis, ETH Zurich, Switzerland, 129 pp., 2009.

Mueller, A. D., Anselmetti, F. S., Ariztegui, D., Brenner, M., Hodell, D. A., Curtis, J. H., Escobar, J., Guilli, A., Grzesik D.A., Guilderson, T.P., Kutterolf, S., and Plötze, M.: Late Quaternary palaeoenvironment of northern

https://doi.org/10.5194/egusphere-2022-787
Preprint. Discussion started: 26 August 2022

Guatemala: evidence from deep drill cores and seismic stratigraphy of Lake Petén Itzá, Sedimentology, 57(5), 1220-1245, https://doi.org/10.1111/j.1365-3091.2009.01144.x, 2010.

Mulder, T., Gillet, H., Hanquiez, V., Reijmer, J. J. G., Droxler, A. W., Recouvreur, A., Fabregas, N., Cavaihes, T., Fauquembergue, K., Blank, D.G. et al.: Into the deep: A coarse-grained carbonate turbidite valley and canyon in ultra-deep carbonate setting, Mar. Geol., 407, 316-333, https://doi.org/10.1016/j.margeo.2018.11.003, 2019

Naeher, S., Gilli, A., North, R. P., Hamann, Y., and Schubert, C. J.: Tracing bottom water oxygenation with sedimentary Mn/Fe ratios in Lake Zurich, Switzerland, Chem. Geol., 352, 125-133, https://doi.org/10.1016/j.chemgeo.2013.06.006, 2013.

Ortega-Guerrero, B., Avendaño, D., Caballero, M., Lozano-García, S., Brown, E. T., Rodríguez, A., García, B., Barceinas, H., Soler, M.A., and Albarrán, A.: Climatic control on magnetic mineralogy during the late MIS 6-Early MIS 3 in Lake Chalco, central Mexico, Quat Sci Rev., 230, 106163, https://doi.org/10.1016/j.quascirev.2020.106163, 2020.

Paillès, C., Sylvestre, F., Escobar, J., Tonetto, A., Rustig, S., and Mazur, J. C.: Cyclotella petenensis and Cyclotella cassandrae, two new fossil diatoms from Pleistocene sediments of Lake Petén-Itzá, Guatemala, Central America, Phytotaxa, 351(4), 247-263, https://doi.org/10.11646/phytotaxa.351.4.1, 2018.

Pérez, L., Frenzel, P., Brenner, M., Escobar, J., Hoelzmann, P., Scharf, B., and Schwalb, A.: Late Quaternary (24–10 ka BP) environmental history of the Neotropical lowlands inferred from ostracodes in sediments of Lago Petén Itzá, Guatemala, J Paleolimnol, 46(1), 59, https://doi.org/10.1007/s10933-011-9514-0, 2011.

Pérez, L., Curtis, J., Brenner, M., Hodell, D., Escobar, J., Lozano, S., and Schwalb, A. Stable isotope values (δ18O & δ13C) of multiple ostracode species in a large Neotropical lake as indicators of past changes in hydrology, Quat Sci Rev. 66(0), 96-111, https://doi.org/10.1016/j.quascirev.2012.10.044, 2013.

Pérez, L., Correa-Metrio, A., Cohuo, S., González, L. M., Echeverria-Galindo, P., Brenner, M., Curtis, J., Kutterolf, S., Stockhecke, M., Schenk, F., Bauersachs, T., and Schwalb, A.: Ecological turnover in neotropical freshwater and terrestrial communities during episodes of abrupt climate change, Quat Res., 101, 26-36, https://doi.org/10.1017/qua.2020.124, 2021.

Peterson, L. C., Haug, G. H., Hughen, K. A., and Röhl, U.: Rapid changes in the hydrologic cycle of the tropical Atlantic during the last glacial, Science, 290 (5498), 1947-1951, https://doi.org/10.1126/science.290.5498.1947, 2000.

R Core Team (2018). R: a language and environment for statistical computing. R Foundation for Statistical Computing, Vienna. https://www.R-project.org

Ramírez-Barahona, S., and Eguiarte, L. E.: The role of glacial cycles in promoting genetic diversity in the Neotropics: the case of cloud forests during the Last Glacial Maximum, Ecol. Evol., 3(3), 725-738, https://doi.org/10.1002/ece3.483, 2013.

https://doi.org/10.5194/egusphere-2022-787
Preprint. Discussion started: 26 August 2022

Reimer, P. J., Austin, W. E., Bard, E., Bayliss, A., Blackwell, P. G., Ramsey, C. B., et al.: The IntCal20 Northern Hemisphere radiocarbon age calibration curve (0–55 cal kBP), Radiocarbon, 62(4), 725-757, https://doi.org/10.1017/RDC.2020.41, 2020.

Rincón-Martínez, D., Lamy, F., Contreras, S., Leduc, G., Bard, E., Saukel, C., Blanz, T., Mackensen, A., and Tiedemann, R.: More humid interglacials in Ecuador during the past 500 kyr linked to latitudinal shifts of the equatorial front and the Intertropical Convergence Zone in the eastern tropical Pacific, Paleoceanography, 25(2), https://doi.org/10.1029/2009PA001868, 2010.

Roy, P. D., Quiroz-Jiménez, J. D., Pérez-Cruz, L. L., Lozano-García, S., Metcalfe, S. E., Lozano-Santacruz, R., López-Balbiaux, N., Sánchez-Zavala J.L., and Romero, F. M.: Late Quaternary paleohydrological conditions in the drylands of northern Mexico: a summer precipitation proxy record of the last 80 cal ka BP, Quat Sci Rev., 78, 342-354, https://doi.org/10.1016/j.quascirev.2012.11.020, 2013.

Royer, A., Malaizé, B., Lécuyer, C., Queffelec, A., Charlier, K., Caley, T., and Lenoble, A.: A high-resolution temporal record of environmental changes in the Eastern Caribbean (Guadeloupe) from 40 to 10 ka BP, Quat Sci Rev., 155, 198-212, https://doi.org/10.1016/j.quascirev.2016.11.010, 2017.

Shackleton, N.J., Fairbanks, R.G., Chiu, T.-C., and Parrenin, F.: Absolute calibration of the Greenland time scale: implications for Antarctic time scales and for D14C, Quaternary Sci. Rev., 23, 1513-1522, https://doi.org/10.1016/j.quascirev.2004.03.006, 2004.

Simmons, C. S., Tarano, J. M. und Pinto, J. H. (Eds.): Clasificacion de reconocimiento de los suelos de la Republica de Guatemala. Ministerio de Agricultura, Guatemala City, Guatemala, 1959.

Svensson, A., Andersen, K. K., Bigler, M., Clausen, H. B., Dahl-Jensen, D., Davies, S. M., Johnsen, S.J., Muscheler, R., Parrenin, F., Rasmussen, S.O., Röthlisberger, R., Seierstad, I., Steffensen, J.P., and Vinther, B. M.: A 60 000 year Greenland stratigraphic ice core chronology, Clim. Past, 4(1), 47-57, https://doi.org/10.5194/cp-4-47-2008, 2008.

Talbot, M. R., and Johannessen, T.: A high resolution palaeoclimatic record for the last 27,500 years in tropical West Africa from the carbon and nitrogen isotopic composition of lacustrine organic matter, Earth Planet. Sci. Lett., 110(1-4), 23-37, https://doi.org/10.1016/0012-821X(92)90036-U, 1992.

Tjallingii, R., Claussen, M., Stuut, J. B. W., Fohlmeister, J., Jahn, A., Bickert, T., Lamy, F., and Röhl, U.: Coherent high-and low-latitude control of the northwest African hydrological balance, Nat. Geosci., 1(10), 670-675, https://doi.org/10.1038/ngeo289, 2008.

Van De Kamp, P. C.: Arkose, subarkose, quartz sand, and associated muds derived from felsic plutonic rocks in glacial to tropical humid climates, J. Sediment. Res., 80(10), 895-918, https://doi.org/10.2110/jsr.2010.081, 2010.

Vriend, M., Groot, M. H. M., Hooghiemstra, H., Bogotá-Angel, R. G., and Berrio, J. C.: Changing depositional environments in the Colombian Fúquene Basin at submillennial time-scales during 284-27 ka from unmixed grain-

https://doi.org/10.5194/egusphere-2022-787
Preprint. Discussion started: 26 August 2022

size distributions and aquatic pollen, Neth J Geosci., 91(1-2), 199-214, https://doi.org/10.1017/S0016774600001591, 2012.

Waelbroeck, C., Pichat, S., Böhm, E., Lougheed, B. C., Faranda, D., Vrac, M., Missiaen, L., Vazquez Riveiros, N., Burckel, P., Lippold, J., Arz, H.W., Dokken, T., and Dapoigny, A.: Relative timing of precipitation and ocean circulation changes in the western equatorial Atlantic over the last 45 kyr. Clim. Past, 14(9), 1315–1330. https://doi.org/10.5194/cp-14-1315-2018, 2018.

Warken, S. F., Vieten, R., Winter, A., Spötl, C., Miller, T. E., Jochum, K. P., Schröder-Ritzrau, A., Mangini, A., and Scholz, D.: Persistent link between Caribbean precipitation and Atlantic Ocean circulation during the Last Glacial revealed by a speleothem record from Puerto Rico, Paleoceanogr Paleoclimatol., 35(11), https://doi.org/10.1029/2020PA003944, 2020

Weltje, G. J. (Ed.): Provenance and dispersal of sand-sized sediments: Reconstruction of dispersal patterns and sources of sand-sized sediments by means of inverse modelling techniques, Utrecht University, The Netherlands, 1994.

Weltje, G. J., and Tjallingii, R.: Calibration of XRF core scanners for quantitative geochemical logging of sediment cores: Theory and application, Earth Planet. Sci. Lett., 274(3-4), 423-438, https://doi.org/10.1016/j.epsl.2008.07.054, 2008.

Weltje, G., Bloemsma, M., Tjallingii, R., Heslop, D., Röhl, U., Croudace, I.: Prediction of Geochemical Composition from XRF Core Scanner Data: A New Multivariate Approach Including Automatic Selection of Calibration Samples and Quantification of Uncertainties, in: Micro-XRF Studies of Sediment Core, edited by: Croudace, I., and Rothwell, R., Springer, Dordrecht, The Netherlands, https://doi.org/10.1007/978-94-017-9849-5_21, 2015.

Wersin, P., Höhener, P., Giovanoli, R., Stumm, W.: Early diagenetic influences on iron transformations in a freshwater lake sediment. Chem. Geol., 90, 233–252., https://doi.org/10.1016/0009-2541(91)90102-W, 1991.

Yarincik, K. M., Murray, R. W., and Peterson, L. C.: Climatically sensitive eolian and hemipelagic deposition in the Cariaco Basin, Venezuela, over the past 578,000 years: Results from Al/Ti and K/Al, Paleoceanography, 15(2), 210-228, https://doi.org/10.1029/1999PA900048, 2000.

Yu S.L., Hamrick J.M., and Lee D. (1984) Wind Effects on Air-Water Oxygen Transfer in a Lake. In: Gas Transfer at Water Surfaces. Water Science and Technology Library, vol 2, edited by: Brutsaert W., and Jirka G.H., Springer, Dordrecht. The Netherlands, https://doi.org/10.1007/978-94-017-1660-4_33, 1984

Zarriess, M., Johnstone, H., Prange, M., Steph, S., Groeneveld, J., Mulitza, S., and Mackensen, A.: Bipolar seesaw in the northeastern tropical Atlantic during Heinrich stadials. Geophys, Res. Lett., 38(4), L04706, https://doi.org/10.1029/2010GL046070, 2011.

Ziegler, M., Nürnberg, D., Karas, C., Tiedemann, R., and Lourens, L. J.: Persistent summer expansion of the Atlantic Warm Pool during glacial abrupt cold events, Nat. Geosci., 1(9), 601-605, https://doi.org/10.1038/ngeo277, 2008.